Plant Stress 15 (2025) 100793

Contents lists available at ScienceDirect

Plant Stress

journal homepage: www.sciencedirect.com/journal/plant-stress

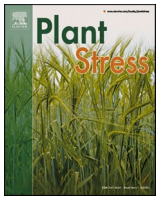

Fungal community dynamics and anthocyanin profiling of grapevine leaves in a vineyard affected by esca

Giovanni Del Frari [a,b,*], Chiara Ingrà [c,1], Marie Rønne Aggerbeck [d,1], Alex Gobbi [e,1,2], Teresa Nascimento [b], Ana Cabral [b], Helena Oliveira [b], Lars Hestbjerg Hansen [e], Alessandra Ferrandino [c], Ricardo Boavida Ferreira [b]

[a] Department of Agricultural, Food, Environmental and Animal Sciences (DI4A), University of Udine, Via delle Scienze 206, 33100 Udine, Italy
[b] LEAF—Linking Landscape, Environment, Agriculture and Food—Research Center, Instituto Superior de Agronomia, Associated Laboratory TERRA, Universidade de Lisboa, Tapada da Ajuda, 1349-017 Lisbon, Portugal
[c] Department of Agricultural, Forestry, Food Sciences (DISAFA), University of Turin, Largo P. Braccini, 2, Grugliasco, Torino 10095, Italy
[d] Department of Environmental Science, Aarhus University, 4000 Roskilde, Denmark
[e] Department of Plant and Environmental Sciences, University of Copenhagen, Thorvaldsensvej 40, 1871 Frederiksberg, Denmark

ARTICLE INFO

Keywords:
Vitis vinifera
Mycobiome
Endophytes
Grapevine trunk diseases

ABSTRACT

Leaves in grapevines affected by esca, a grapevine trunk disease, may occasionally manifest a symptom known as the 'esca leaf stripe symptom.' Most frequently, this symptom appears as scorching in the interveinal tissue, with red pigmentation observed between scorched and healthy tissue. However, purple pigmentation or an absence of pigmentation is occasionally reported. The synthesis and accumulation of anthocyanins may drive these different symptom phenotypes. Recent evidence also implicates fungal endophytes in host manipulation, potentially influencing grapevine metabolic profiles, including anthocyanins. In this study, working on cultivars Cabernet Sauvignon and Touriga Nacional, we used DNA metabarcoding (i) to explore the microbial dynamics of endophytes during symptom progression in esca-affected leaves, and (ii) to reveal the fungal diversity for different symptom phenotypes, along with their qualitative and quantitative anthocyanins composition.

The endophytic mycobiome profiling revealed a large fungal richness (260 taxa), and a beta diversity influenced by cultivar ($P < 0.01$) and vintage ($P = 0.001$). We observed significant differences in beta diversity between leaves affected by chlorotic spots and asymptomatic ones ($P < 0.05$), revealing major shifts in fungal community composition during early stages of esca symptom progression. Comparing asymptomatic leaves and different symptom phenotypes, we detected cultivar and vintage-dependent alterations in alpha and beta diversity, as well as in individual taxa abundance (e.g. *Botrytis caroliniana* over-represented in red leaves). Total anthocyanin accumulation was influenced by cultivar ($P \leq 0.0001$) but not by vintage. In Touriga Nacional, and to a lesser extent in Cabernet Sauvignon, purple leaves accumulated significantly lower amounts of trihydroxylated anthocyanins and acyl-derivatives, when compared to red leaves.

Fungal communities significantly alter in composition during esca symptom progression, and for different symptom phenotypes, suggesting a strong correlation between microbial structure and the physiological and biochemical processes that occur in leaves.

1. Introduction

Charming to the eye, yet a sign of doom, the esca leaf stripe symptom is one of the least understood aspects of the esca complex of diseases (Del Frari et al., 2022; Del Frari et al., 2021; Lecomte et al., 2012) (Fig. 1). Symptomatic grapevines (*Vitis vinifera* L.) are currently included in the syndromes grapevine leaf stripe disease (GLSD) and esca proper, depending on wood symptomatology and fungal pathogens found in perennial organs (Surico, 2009; Mondello et al., 2018). Typical wood symptoms found in grapevines manifesting the esca leaf stripe symptom,

* Corresponding author.
E-mail address: gdelfrari@isa.ulisboa.pt (G. Del Frari).
[1] These authors contributed equally to the study.
[2] Current affiliation: European Food and Safety Authority (EFSA), Via Carlo Magno 1A, 43126 Parma, Italy.

https://doi.org/10.1016/j.stress.2025.100793
Received 9 October 2024; Received in revised form 21 January 2025; Accepted 2 March 2025
Available online 3 March 2025

also known as 'tiger stripes', are brown wood streaking, cankers, and, most frequently, white rot (Del Frari et al., 2021; Surico, 2009; Mugnai et al., 1999; Gramaje et al., 2018), which lead to losses in plant vigor, yield quantity and quality, and premature plant death (Fontaine et al., 2016). Interestingly, not all wood-symptomatic vines manifest tiger stripes. In GLSD and esca proper-affected vines, the leaf stripe symptom is known to appear discontinuously, from year to year; its onset may occur over an extended period of time, between late spring and mid-summer; it may affect the whole canopy or only portions of it, *e.g.* single shoots, multiple shoots on the same spur or an entire arm (Lecomte et al., 2012; Del Frari et al., 2019; Serra et al., 2018). Moreover, numerous variables influence symptoms onset and severity, such as biotic and abiotic factors, and agricultural practices (Del Frari et al., 2021). Overall, this suggests that wood symptoms and their causal agents are not the sole responsible for tiger stripes, but they are only one piece of the puzzle. This conclusion is further supported by the overwhelming lack of success in past attempts of reproducing symptoms by artificial inoculations with esca-associated fungi, with only a few exceptions (e.g. Del Frari et al., 2021), and by the controversy that still surrounds the identity of the leaf stripe symptom triggering factor(s) (Del Frari et al., 2022; Del Frari et al., 2021). The microbiological aspect of perennial organs in grapevines manifesting tiger stripes and the available control strategies to mitigate symptoms incidence and severity have been recently reviewed in Del Frari et al. (2022), Del Frari et al. (2021).

A yet unexplored aspect of symptomatic leaves concerns three symptom phenotypes that may manifest in GLSD or esca-affected grapevines (Fig. 1). The similarities among them are the interveinal necrotic lesions and the green lamina portions in proximity of the main veins, while the differences concern symptom onset, progression and the lamina pigmentation between necrotic lesions and green tissue.

(1) Esca tiger stripes is the most frequently observed symptom phenotype in vineyards, and the first described in the scientific literature (Mugnai et al., 1999; Viala, 1926). Phenotypic alterations in leaves start with the appearance of scattered chlorotic spots that may expand and coalesce (Fig. 1, C). Subsequently, necrotic lesions appear in correspondence of some chlorotic spots and portions of the lamina surrounding chlorotic tissue acquire pigmentation (Fig. 1, II, D), typically described as tonalities of red (Lecomte et al., 2012; Surico, 2009; Mugnai et al., 1999; Serra et al., 2018). Leaf margins may or may not turn necrotic and interveinal lesions may coalesce or remain of constant size throughout the growing season (Lecomte et al., 2012).

(2) In apoplectic leaves, portions of interveinal tissue undergo a rapid phase of discoloration, turning pale green to gray, they necrotize (Fig. 1, III), and wilt. After necrotizing, affected shoots typically lose all leaves in a matter of days (Lecomte et al., 2012; Spagnolo et al., 2012; Magnin-robert et al., 2017). Alterations in the pigmentation of the lamina between necrotic lesions and green tissue -in proximity of the main veins- are minimal or absent, although a thin violet strip is occasionally observed bordering the necrotic tissue.

(3) In 2001, Larignon and colleagues brought attention over the black dead arm (BDA) syndrome, a putative grapevine wood disease caused by *Botryosphaeriaceae* fungi, characterized by esca leaf stripe-like phenotype (Larignon et al., 2001; Larignon and Dubos, 2001). In this third symptom phenotype, symptoms manifest earlier in the season, when compared to esca tiger stripes, and they appear as wine-red to purple areas on the margins and interveinal areas of the lamina. Subsequently, necrotic lesions appear in correspondence of some pigmented areas and may coalesce similarly to esca tiger stripe. Necrotic lesions remain surrounded by varying proportions of wine-red to purple tissues, which divide them from green tissues, localized in proximity of the main veins (Fig. 1, I) (Lecomte et al., 2012; Larignon et al., 2001; Úrbez-Torres, 2011; Kuntzmann et al., 2010). In addition, researchers detected metabolic, cytological and histological differences between BDA and esca leaves (Valtaud et al., 2009; Valtaud et al., 2011), or associated canes (Fleurat-Lessard et al., 2013). However, over the following years, multiple authors challenged the view that the BDA syndrome is distinct from esca, bringing forward three main issues: (i) the BDA phenotype may occasionally transition to esca phenotype during the growing season; (ii) in red varieties, esca tiger stripes may exhibit a broad range of coloring patterns, and it is possible – albeit infrequent – to find both wine-red to purple and tonalities of red pigmentation on the same leaf or on different leaves on the same shoot; (iii) the

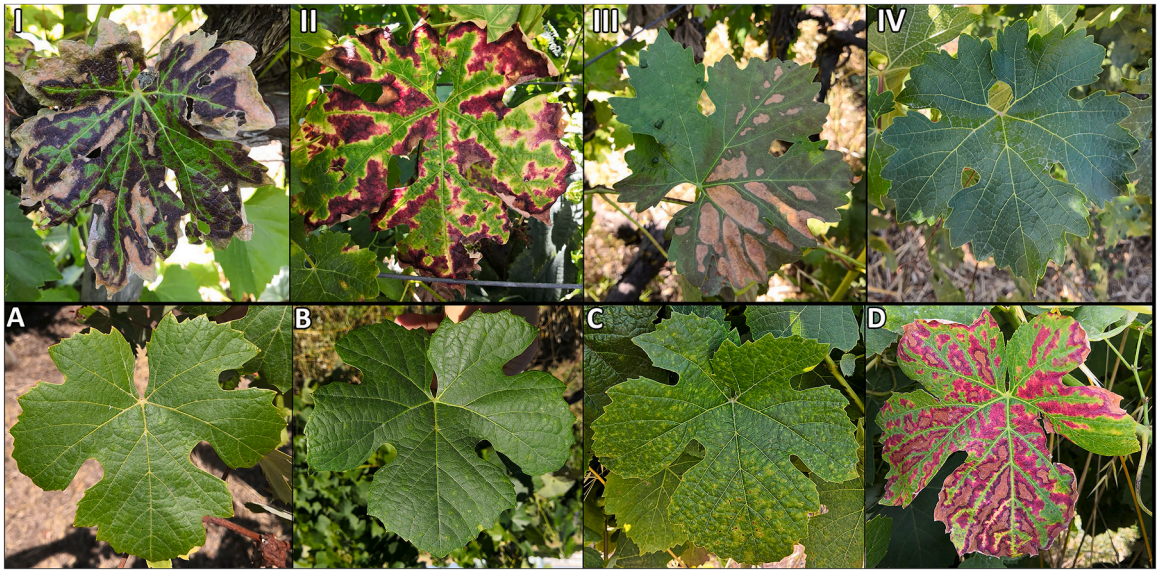

Fig. 1. Grapevine leaves (cv. Cabernet Sauvignon) manifesting different symptom phenotypes (I, II, and III), and asymptomatic leaves (phenotype IV; Asy). Phenotype I is identified as BDA (black dead arm, *sensu* Larignon (Larignon et al., 2009)), phenotype II as Esca / esca tiger stripes, and phenotype III as apoplectic leaves (Apox). Grapevine leaves (cv. Touriga Nacional) in asymptomatic shoots, sampled between the fifth and seventh internode (A; YAsy), and two internodes below (B; Asy); in symptomatic shoots, sampled between the fifth and seventh internode, affected by scattered chlorotic spots (C; Chl), and two internodes below, Esca leaves (D).

BDA phenotype has not been entirely reproduced by artificial inoculation with putative BDA-associated fungi (Lecomte et al., 2012; Úrbez-Torres, 2011; Kuntzmann et al., 2010; Lecomte et al., 2006; Surico et al., 2006). For these reasons, the BDA phenotype is currently included in the cluster of symptoms manifested in esca-affected grapevines, therefore not a separate syndrome, yet, experimental evidence explaining the observed differences in pigmentation, symptom onset and progression is still missing.

A significant body of research has been carried out to assess anatomical, physiological, gene expression, and metabolomic alterations occurring in tiger striped leaves (Magnin-robert et al., 2017; Valtaud et al., 2011; Lima et al., 2010; Goufo and Cortez, 2020; Goufo and Singh, 2021; Magnin-Robert et al., 2011; Calzarano et al., 2016; Calzarano et al., 2021; Weiller et al., 2024; Bortolami et al., 2023). However, the microbiological aspect has been largely neglected. While it is known that esca-associated pathogens are not found in symptomatic leaves (Mugnai et al., 1999), the role of the endophytic mycobiome and its interaction with grapevine leaf physiological and biochemical processes remains to be evaluated. In a recent paper, Chen *et al.* (2020) identified multiple fungal taxa over- or under-represented in differently colored grapevine leaves, suggesting a potential correlation between microbiota and total anthocyanins (Chen et al., 2020). Anthocyanins are secondary metabolites responsible for berry pigmentation (Castellarin et al., 2006; Castellarin and Di Gaspero, 2007); they can also accumulate in vegetative organs, mainly leaves, as a line of defense against environmental stress, such as exposure to high light radiation (Tattini et al., 2005; Tattini et al., 2014), to protect chloroplasts and to reduce the incidence of photo-oxidative stress (Lev-Yadun and Gould, 2008; Feild et al., 2001). In leaves, anthocyanins are accumulated in the cytosol and stored in the vacuole of epidermal and/or mesophyll cells (Kedrina-okutan et al., 2018; Flamini et al., 2013; Hatier and Gould, 2008), but their localization may change during leaf ontogenesis (Merzlyak et al., 2008). In addition, anthocyanins are involved in grapevine-pathogen interactions: they are absent in adult and healthy leaf blades (Kedrina-okutan et al., 2018), whereas they may accumulate in large amounts after pathogen attack, like in the case of *flavescence dorèe* and *bois noir* phytoplasmas, and grapevine leafroll-associated virus (Margaria et al., 2014; Negro et al., 2020; Gutha et al., 2010). Moreover, anthocyanins accumulate at specific developmental stages and/or during physiological changes, such as leaf senescence (Hoch et al., 2001; Matus et al., 2017). In fact, a popular hypothesis is that anthocyanins are the end products of leaf senescence because of the overflow of carbohydrates during the recovery of photosynthetic products (Feild et al., 2001).

Fungal endophytes are known to manipulate their host (Collinge et al., 2022; Dupont et al., 2015; Giauque et al., 2019), and recent evidence revealed endophyte-dependent alteration in metabolic (Pan et al., 2020) and anthocyanin (Yu et al., 2020) profiles in grapevine leaves and other crops (Ważny et al., 2021; de Vries et al., 2018). In an attempt of clarifying the involvement of grapevine leaf fungal endophytes and anthocyanins in the three symptom phenotypes described above, we set three main objectives. (1) – To characterize the endophytic mycobiome of grapevine leaves using DNA metabarcoding (next-generation sequencing; NGS); (2) – To assess the microbial dynamics during the progression of esca tiger stripes, from scattered chlorotic spots to fully symptomatic leaves. (3) – To explore fungal community composition, anthocyanin concentration and profile, and the relationship between the two, when comparing different symptom phenotypes and asymptomatic leaves.

2. Materials and methods

2.1. The vineyard, field sampling, and samples processing

2.1.1. The vineyard

Field sampling took place in the experimental vineyard (Almotivo) of the Instituto Superior de Agronomia, University of Lisbon, Lisbon, Portugal (38°42′32.7″N, 9°11′11.5″W). The vineyard has a density of 3333 plants/ha, the soil is classified as vertisol, it is managed under conventional agricultural practices and rainfed. The selected cultivars were Cabernet Sauvignon, known for its high susceptibility to grapevine trunk diseases (Gastou et al., 2024; Csótó et al., 2023) and Touriga Nacional, a less susceptible cultivar, both grafted on 140 Ruggeri rootstock (*Vitis berlandieri* × *Vitis rupestris*), trained as bilateral cordon Royat and spur-pruned. Grapevines were planted in 1998, and they were 22 and 23 years-old at the time of sampling. The vineyard has a history of esca, with leaf-symptomatic grapevines accounting for ≤1 % of the total plants in all recorded years (from 2015 to 2022). An in-depth microbiological analysis of fungal endophytic communities detected in cv. Cabernet Sauvignon can be found in Del Frari et al. (2019) and Del Frari et al. (2023). Symptoms correlated to other grapevine trunk diseases were also detected (Vaz et al., 2020).

2.1.2. Field sampling

Sampling took place on June 23rd, 2020, and on June 17th, 2021, at the phenological stage of 'pea-sized' berries, at the beginning of the seasonal manifestation of symptoms. Plant protection products (Pergado F, Syngenta, 5 % Mandipropamid + 40 % Folpet; Indar 5EW, Dow, 4.95 % Fenbuconazole) were sprayed three (2020) or two (2021) weeks before sampling. Due to symptom discontinuity, individual grapevines sampled in 2021 were not the same sampled on the previous year.

To address Objective 2, we examined cvs Cabernet Sauvignon and Touriga Nacional, in 2020. We established four categories, based on symptomatology and leaf age (Fig. 1, A - D). On asymptomatic shoots, we sampled (A) – 'Young asymptomatic leaves' (YAsy), between the fifth and seventh internode, and (B) – 'Asymptomatic leaves' (Asy), two internodes below YAsy leaves. On symptomatic shoots, we sampled (C) – leaves affected by 'scattered chlorotic spots' (Chl), between the fifth and seventh internode, and (D) – 'Esca leaves' (Esca), characterized by interveinal necrosis followed by chlorotic, red and green tissues, two internodes below Chl leaves. The term 'Esca' (with a capital E) is used in the text specifically for the leaf symptoms just described, as opposed to 'esca', which refers to the disease complex. Asymptomatic shoots were monitored throughout the growing season to confirm that leaves remained asymptomatic.

To address Objective 3, we examined cvs Cabernet Sauvignon and Touriga Nacional, both in 2020 and 2021. Symptomatic and asymptomatic leaves were collected between the third and fifth internode and, at the time of sampling, approximately 10–25 % of the surface area of the symptomatic leaf blade presented necrotic lesions. We established four categories based on leaf symptom phenotypes (Fig. 1, I - IV). (I) – 'BDA leaves' (BDA), *sensu* Larignon (Larignon et al., 2009), characterized by interveinal necrosis followed by dark purple and green tissues; (II) – 'Esca leaves', as described above (Objective 2, category D); (III) – 'Apoplectic leaves' (Apox), characterized by interveinal necrosis followed by green tissue; (IV) – 'Asy leaves', as described above (Objective 2, category B). Overall, from the day of sampling, Esca and BDA leaves persisted on the shoots for at least two weeks, while Apox leaves withered and fell within one week. Apox leaves were sampled exclusively in 2020, as this symptom phenotype was not detected in 2021. In Esca leaves (symptom phenotype II), chlorotic tissue was less evident/absent in cv. Touriga Nacional, while always present in cv. Cabernet Sauvignon (Fig. 1, II, D). At the time of sampling, there were no visible symptoms of a leaf pathogen infection (e.g. downy or powdery mildews) or mineral deficiency.

For each of the above-mentioned categories (Objectives 2 and 3), we

collected between 8 and 12 biological replicates, each of them corresponding to leaves sampled from a single shoot, on a single vine. While in the field, sampled leaves were stored in ice, in sterile plastic bags, and then moved to a −80 °C freezer until sample processing.

2.2. Sample processing, DNA extraction, library preparation and sequencing

Leaves were deprived of necrotized tissue with the use of sterile scissors and they were surface sterilized to remove epiphytes, following a procedure similar to that described in Fan et al. (2020). Briefly, for each category, all biological replicates underwent double rinsing in sterile distilled water followed by immersion in a solution of sodium hypochlorite 3 % (v/v) for 5 min, followed by a triple rinse in sterile distilled water. Aliquots of the water from the last rinse were plated on potato dextrose agar and incubated at 25 °C, in the dark, for two weeks to confirm the absence of microbial growth.

After sample processing, five surface sterilized leaves per each category*cultivar*year were ground to dust using sterile mortars and pestles with the aid of liquid nitrogen. Aliquots of 0.15 g from each ground biological replicate were used for DNA extraction. This step was performed by combining the method described in Cenis (1992) and the ZymoBIOMICS™ DNA Miniprep Kit. Briefly, in lysis tubes, we added leaf sample and extraction buffer as in Cenis (1992), we then processed the samples in a bead beater fitted on a vortex for 10 min followed by heating at 65 °C for 10 min. The DNA extraction protocol was then followed as per (Cenis, 1992) up until the DNA precipitation step, which was followed by DNA binding, washing, and elution steps as described in ZymoBIOMICS™ manufacturer instructions. Two negative controls of the DNA extraction procedure were added.

The amplicon chosen in this study targets the internal transcribed spacer region 1 (ITS1), and the primer set selected was ITS1F2 – ITS2 with overhang recommended by Illumina. The full sequence of the primers, including Illumina overhangs, is the following: ITS1F2 (5′-TCGTCGGCAGCGTCAGATGTGTATAAGAGACAG-GAACCWGCGGARGGATCA-3′) and ITS2 (5′-GTCTCGTGGGCTCGGAGATGTGTATAAGAGACAG-GCTGCGTTCTTCATCGATGC-3′) (Gaylarde et al., 2017). For building libraries, we used a double-step PCR approach as reported by Feld et al. (2015). Each first-step PCR reaction contained 12.5 μL of Supreme NZYTaq II 2x Green Master Mix™ (NZYtech™), 0.5 μL of forward and reverse primers from a 10 μM stock, 1.5 μL of sterile water, and 5 μL of template. Each reaction was pre-incubated at 95 °C for 2 min, followed by 39 cycles of 95 °C for 15 s, 55 °C for 15 s, 72 °C for 40 s; a further extension was performed at 72 °C for 10 min. Second PCR-step for barcoding, fragment-purification by using MagBio beads, and Qubit quantification was performed as reported in Gobbi et al. (2019). Final pooling was performed at 10 ng/sample.

DNA Sequencing was performed using an in-house Illumina® MiSeq instrument and 2 × 250 paired-end reads with V2 Chemistry.

2.3. Bioinformatics

Data produced by sequencing have been demultiplexed using our Illumina® Miseq platform. Demultiplexed reads were analyzed using QIIME2 v 2022.2 (Caporaso et al., 2010) with an analogous pipeline described in Gobbi et al. (2019). To summarize the data processing, raw reads were clipped to 12 bp on the 5′ end removing the primers. The reads were then denoised using DADA2 (Callahan et al., 2017) discarding singletons. In order to reduce the effect of low-abundant amplicon sequence variants (ASVs), on downstream statistical analysis, any feature appearing <25 times in the complete dataset was filtered out. Taxonomical assignment was performed at 99 % identity through the plugin QIIME feature classifier (Bokulich et al., 2018) using BLAST and the UNITE (Koljalg et al., 2013) v9 database for ITS. If taxonomy was not assigned with reasonable precision, further attempts were performed on the dominant features, using BLAST against the NCBI database to confirm or refine the result.

The raw data of this study is available in the European Nucleotide Archive (ENA accession number PRJEB80528).

2.4. Sample processing and quantitative analyses of anthocyanins by HPLC-DAD

Leaves deprived of necrotic tissue were freeze-dried. Anthocyanins were extracted from lyophilized leaves (0.5 mg) in 25 mL of pH 3.9 hydroalcoholic buffer (40 % v/v ethanol, 2 g/L Na2S2O5, 5 g/L tartaric acid, 22 mL/L 1 N NaOH) and left to macerate for a week at −20 °C. The samples were centrifuged for 10 min at 4000 rpm. The supernatant was separated and kept in the dark, the pellet was resuspended in the same buffer, and then centrifuged again. The two extracts were mixed and brought to a final volume of 50 mL. Extracts were stored at −20 °C until further analysis.

Leaf extracts were retained on a Sep-Pak C18 silica-based bonded phase cartridge (Waters Corp., WAT051910, Milford, MA) eluted with methanol. The extracts were evaporated to dryness in a rotary evaporator (Laborota 4000, Heidolph Instruments GmbH & Co. KG, Schwabach, Germany), and then were resuspended with solvent B for HPLC and filtered through 0.20 μm membrane filter GHP Acrodisc (PALL Italia, Buccinasco, Milano, Italy).

Samples were analyzed by high-performance liquid chromatography (HPLC) with an Agilent 1260 (Agilent, Waldbronn, Germany), equipped with a diode array detector (DAD) detector (G1316A) with a reverse-phase column Purosphere STAR RP-18 end-capped (5 μm) packed into LiChroCART 250-4 HPLC—Cartridge (25 cm × 0.4 cm ID; Merck KGaA, Germany) with a guard column LiChroCART 4-4 of the same packing material. DAD detector was set at 520 nm. Solvent A was 10 % (v/v) formic acid and solvent B was water/methanol/formic acid (40:50:10, v/v/v). The chromatographic separation was carried out at a flow rate of 1 mL/min with a gradient from 28 % to 72 % of B in 63 min, with the following gradient of solvent A: from 72 to 55 % in 15 min; to 30 % in 20 min; to 10 %, in 10 min; to 1 % in 10 min; to 72 % in 5 min and holding 72 % for 3 min. Results were expressed as mg of malvidin 3-O-glucoside chloride equivalent per kg of leaves dry weight.

The profile of anthocyanins was identified based on their UV–VIS spectra and retention times by comparison with standards. Malvidin-, peonidin-, petunidin-3-O-glucoside chloride, myrtillin chloride (delphinidin-3-O-glucoside chloride) and kuromanin chloride (cyanidin-3-O-glucoside chloride) were purchased from Extrasynthèses (Lyon, Genay Cedex, France). Acylated anthocyanin, not available as pure standard molecules, were tentatively identified on the basis of previous studies conducted on the leaf anthocyanin extracts of V. *vinifera* cultivars by HPLC-ESI-MS/MS (Kedrina-okutan et al., 2018) and based on the current laboratory identification of acyl-derived anthocyanin in grapes. Since anthocyanins acyl-derivatives were tentatively identified, we did not consider them separately but we summed the individual peak areas and calculated their concentration and their relative percentage incidence over total anthocyanins. A tentative identification is found in supplementary materials (Table S1), where average retention times of individual peaks in the described chromatographic conditions are reported.

2.5. Statistical analyses and data visualization

2.5.1. Data analysis for NGS

The frequency table and its taxonomy were combined, converted to biom format in QIIME (Caporaso et al., 2010), then merged with a table of metadata into an S4 object and analyzed in R (version 3.6.3). The 'phyloseq' (version 1.30.0) (McMurdie and Holmes, 2013) and 'biomformat' (version 1.14.0) (McMurdie and Paulson, 2016) packages were used to create the primary data object. The 'vegan' (version 2.5.5) (Oksanen et al., 2013), 'mvabund' (version 4.1.3) (Wang et al., 2017), 'metacoder' (version 0.3.4) (Foster et al., 2017), 'taxa' (version 0.3.4)

(Foster et al., 2018), 'tidyverse' (version 1.3.0) (Wickham et al., 2019), 'microbiome' (version 1.8.0) (Lahti and Sudarshan), ggplot2, (version 3.3.2) (Valero-Mora, 2015), 'pairwiseAdonis' (version 0.4.1) (Arbizu, 2020), 'gridExtra' (version 2.3), and directlabels (version 2024.1.21) packages were used for data manipulation, visualization, and statistical analysis. The R code used for these analyses is publicly available at https://github.com/Marieag/LeaSyBiome/blob/main/LeaSyBiome_Study1.R.

The alpha diversity was measured using the Simpson's (D) and inverse Simpson's (1/D) diversity indexes and tested with one-way ANOVA with a post hoc Bonferroni correction to determine significant differences between cultivars (Cabernet Sauvignon, Touriga Nacional), year (2020 and 2021), and between leaf symptoms (BDA, Esca, Apox and Asymptomatic leaves).

We analyzed the β-dispersion to measure between-sample variances in abundance, computing the distances of group members to the group centroid. The resulting ordination was plotted using a Bray-Curtis distance matrix. To assess overall inter-group variance (beta diversity) for each year and cultivar, we also performed permutational multivariate analysis of variance (PERMANOVA) with 999 permutations, using the "vegan" package. Post hoc pairwise tests were performed to evaluate the differences between categories using the "pairwiseAdonis" wrapper, applying FDR to correct for multiple comparisons.

Relative abundance for each taxon was calculated and visualized using barplots.

Additionally, we generated heat trees to visualize effect size of the relative abundance of fungal taxa at different taxonomic levels using the 'MetacodeR' package, which calculates the log2 fold change (LfC) in genus and family abundance. A Wilcoxon Rank Sum test was applied to test differences between the same species in different categories, and the resulting p-values were corrected for multiple comparisons using FDR, as implemented in MetacodeR. We focused our analysis on taxa present at RA>0.1 %, and P-value threshold was set to 0.05.

2.5.2. Data analysis for anthocyanins

All data were analyzed by RStudio Build 372 software program version for Windows. Analysis of variance was performed by two-way ANOVA, normalizing data with $\log_{10}$, and followed by Bonferroni post-hoc test at $P \leq 0.05$, $P \leq 0.01$, $P \leq 0.001$, and $P \leq 0.0001$. All measurements were performed in triplicates, and results were expressed as means ± standard errors.

2.5.3. Data visualization for NGS and anthocyanins

Finally, we correlated anthocyanin levels with microbial presence by overlaying anthocyanin level contours on top of samples and fungal taxa, based on a Bray-Curtis dissimilarity matrix.

The ordisurf function was utilized to visualize potential relationships between anthocyanin levels and fungal species presence in grapevine leaves (McCaig et al., 2024; Yang et al., 2022). This fits a smooth surface to environmental data over a pre-existing ordination plot, using a generalized additive model (GAM) to create contour lines representing the variation of the environmental variable—in this case, total anthocyanin levels—across the ordination space.

3. Results

3.1. Sequencing dataset description

A total of 96 samples were sequenced, 90 representing samples included in the study and the remaining 6 resulting from the DNA sequencing of negative controls for the DNA extraction ($n = 3$) and PCR ($n = 3$). After denoising the raw reads removing singletons and low abundant features, the sequencing dataset used for the analysis consist in 90 samples and contains a total of 2.638.250 denoised reads. These reads are represented by 1424 unique features. All samples included in this study were retained while the negative controls were discarded due to insufficient number of reads.

3.2. Endophytic mycobiome overview – objective 1

When looking at the total dataset (objective 1), the microbial composition of endophytic fungi in grapevine leaves, in terms of taxa assigned to the different features, corresponds to 260 taxa. Among them, 56 were assigned to genus level (21.5 %), and 174 to species level (67 %). Ten taxa are detected at a relative abundance (RA) greater than 1 %, corresponding to 85 % of the total dataset RA, 21 taxa at a RA between 1 and 0.1 %, and 229 are considered rare taxa (RA<0.1). Among non-rare taxa (i.e. RA>0.1 %), those identified to genus and/or species level are listed in Table 1.

Ascomycetes are dominant (54.9 %), followed by oomycetes (29.1 %) and basidiomycetes (6.9 %). The most abundant families are *Peronosporaceae* (29.1 %), *Cladosporiaceae* (18.1 %), *Pleosporaceae* (13.9 %), *Aureobasidiaceae* (12.5 %), and *Debaryomycetaceae* (6.6 %). Among the RA>1 % taxa, the most abundant are *Plamopara viticola, Cladosporium delicatulum, Aureobasidium* sp., *Debaryomyces* sp. and *Stemphylium* sp., the former being the only known pathogen affecting grapevine leaves. Three taxa are reported for the first time in grapevine, namely *Botrytis caroliniana, Pyrenophora chaetomioides and Daldinia raimundi* (Table 1). GTD-associated fungi were not detected among non-rare taxa. However, small abundances (RA<0.01 %) of *Diplodia, Phaeomoniella chlamydospora, Fomitiporia* and *Neofusicoccum* are present in the dataset.

In adult leaves of different categories, i.e. three symptom phenotypes and asymptomatic (dataset for objective 3), all non-rare taxa are found both in Cabernet Sauvignon and in Touriga Nacional. Taxa *Plasmopara*

Table 1
Taxonomic classification and relative abundances (RA) of non-rare taxa (RA>0.1 %) in the total dataset, identified at genus or species level.

Phylum (RA, %)	Family (RA, %)	Genus/Species	RA (%)
Oomycetes (29.1)	*Peronosporaceae* (29.1)	*Plasmopara viticola*	29.1
	Cladosporiaceae (18.1)	*Cladosporium delicatulum*	17.6
		Cladosporium ramotenellum	0.5
	Aureobasidiaceae (12.5)	*Aureobasidium* sp.	9.9
		Aureobasidium pullulans	2.6
		Stemphylium sp.	7.5
		Alternaria sp.	3.7
	Pleosporaceae (13.9)	*Alternaria infectoria*	1.9
		Alternaria metachromatica	0.5
		Paradendryphiella arenariae	0.2
		Pyrenophora chaetomioides †	0.1
	Debaryomycetaceae (6.6)	*Debaryomyces* sp.	6.6
	Sclerotiniaceae (1.2)	*Botrytis caroliniana* †	1.2
Ascomycetes (54.9)	*Mycosphaerellaceae* (0.8)	*Mycosphaerella tassiana*	0.8
	Didymellaceae (0.9)	*Epicoccum nigrum*	0.8
		Didymella sp.	0.1
	Didymosphaeriaceae (0.3)	*Pseudopithomyces chartarum*	0.3
	Phaeosphaeriaceae (0.2)	*Sclerostagonospora lathyri*	0.2
	Xylariaceae (0.2)	*Daldinia raimundi*†	0.2
	Periconiaceae (0.1)	*Periconia byssoides*	0.1
	Saccharomycetaceae (0.1)	*Hanseniaspora guilliermondii*	0.1
	Sporidiobolaceae (5.1)	*Sporobolomyces roseus*	4.9
		Sporobolomyces oryzicola	0.2
Basidiomycetes (6.9)	*Filobasidiaceae* (1.6)	*Filobasidium* sp.	0.9
		Filobasidium chernovii	0.7
	Bulleribasidiaceae (0.2)	*Vishniacozyma* sp.	0.2

† first report in grapevine.

viticola, Botrytis caroliniana and *Alternaria infectoria* are over-represented in Cabernet Sauvignon (2-fold difference or more), while *Aureobasidium* sp., *Epicoccum nigrum* and *Filobasidium chernovii* are more abundant in Touriga Nacional. When examining vintages, all non-rare taxa are found both in 2020 and 2021, exception for taxon *Aureobasidium pullulans*, detected exclusively in year 2020. Vintage-wise, numerous taxa are differentially abundant (at least 3-fold difference), some of them being *P. viticola* and *F. chernovii,* over-represented in 2020, and *Debaryomyces* sp., *Cladosporium ramotenellum* and *E. nigrum*, more abundant in 2021.

3.3. Mycobiome and Esca symptoms progression in leaves – objective 2

3.3.1. Alpha and beta diversity

The alpha diversity, measured using Simpson and InvSimpson indices, does not vary between leaf age groups, although a strong trend suggests differences when comparing cultivars ($P = 0.051$). In Cabernet Sauvignon, the Simpson index varies significantly when comparing young asymptomatic leaves (YAsy) and Esca leaves ($P = 0.012$), while strong trends are observed when comparing asymptomatic leaves (Asy) and Esca, and YAsy and leaves affected by chlorotic spots (Chl, $P = 0.06$). Concerning the InvSimpson index, trends are observed when comparing Asy and YAsy leaves with Esca (Fig. 2). In Touriga Nacional, neither significant differences nor trends are observed for both examined indices.

The beta dispersion varies between leaf age groups ($P = 0.001$). Significant variation is evident when comparing the four leaf categories, both in Cabernet Sauvignon ($P = 0.014$) and Touriga Nacional ($P = 0.002$). In Cabernet Sauvignon, the clustering pattern reveals that Esca and Chl leaves diverge from YAsy leaves ($P = 0.051$), and a strong trend of divergence separates Esca and Asy leaves ($P = 0.056$) (Fig. 2). A similar pattern is observed in Touriga Nacional, where significant differences are found when comparing YAsy leaves with all other leaf categories ($P \leq 0.047$), and Chl with Asy leaves ($P = 0.042$). In both cultivars, no differences in clustering are observed when comparing Esca and Chl leaves ($P > 0.05$).

3.3.2. Taxa abundance

The qualitative and quantitative microbial composition varies when comparing cultivars and leaf categories (Figs. 3 and 4).

When comparing young asymptomatic leaves (YAsy) and leaves affected by chlorotic spots (Chl), both in Cabernet Sauvignon and Touriga Nacional, *Sporobolomyces roseus, Filobasidium* sp., *Aureobasidium* sp. and *Epicoccum nigrum* are more abundant in Chl leaves, while no taxa are over-represented in YAsy leaves.

When comparing Chl and Esca leaves, in both cultivars, only *E. nigrum* and, to a lesser extent, *Alternaria infectoria* are more abundant in the former, while only *Debaryomyces* sp. is moderately over-represented in the latter.

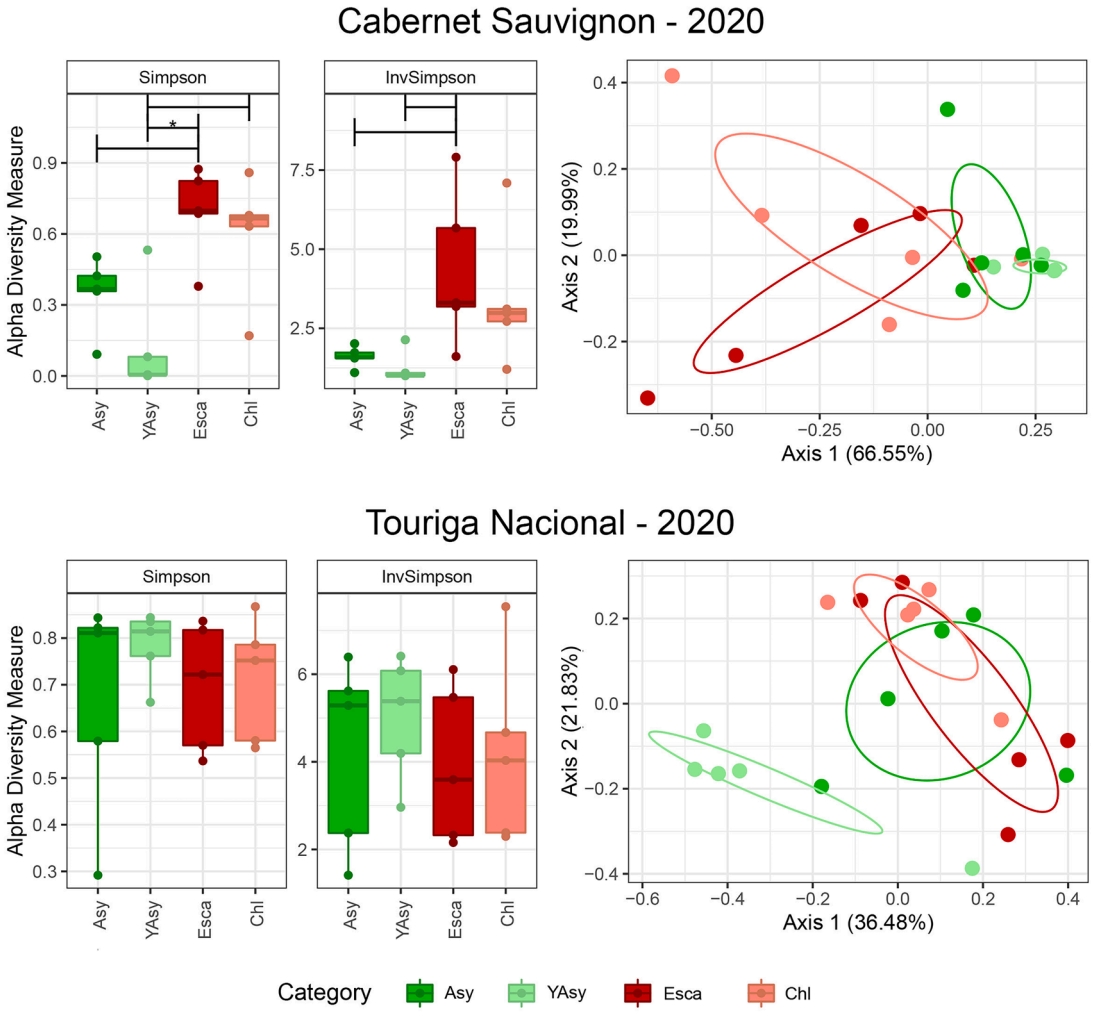

Fig. 2. Box plots of alpha diversity indices (Simpson and InvSimpson) and PCoA plots of beta dispersion based on the Bray–Curtis dissimilarity of the fungal communities in different leaf categories (Asy, YAsy, Esca, Chl) in grapevine cvs. Cabernet Sauvignon and Touriga Nacional, in 2020. The horizontal brackets marked with an asterisk (*) indicate statistical differences, according to a one-way ANOVA with a post hoc Bonferroni correction, while brackets without asterisks indicate trends ($0.10 < P < 0.05$). Ellipses illustrate the multivariate normal distribution of samples within the same leaf category.

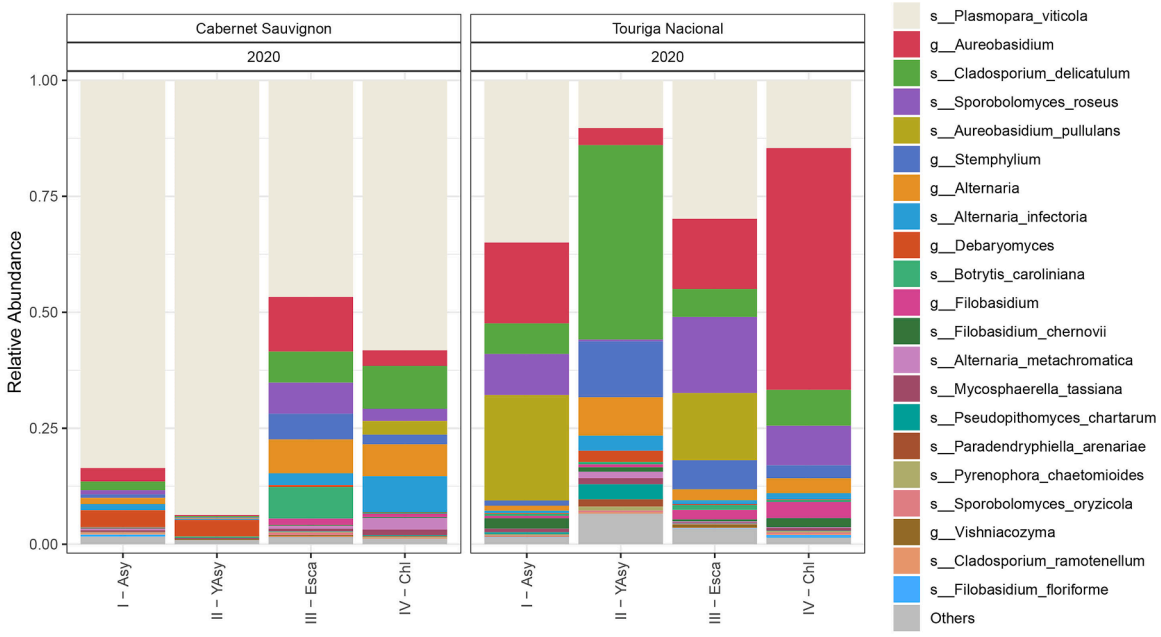

Fig. 3. Bar plots of the relative abundance of the 21 most abundant taxa identified at the genus (g_) or species (s_) level found in different leaf categories (Asy, YAsy, Esca, Chl), in grapevine cvs. Cabernet Sauvignon and Touriga Nacional, in 2020. 'Others' are taxa not included among the 21 most abundant.

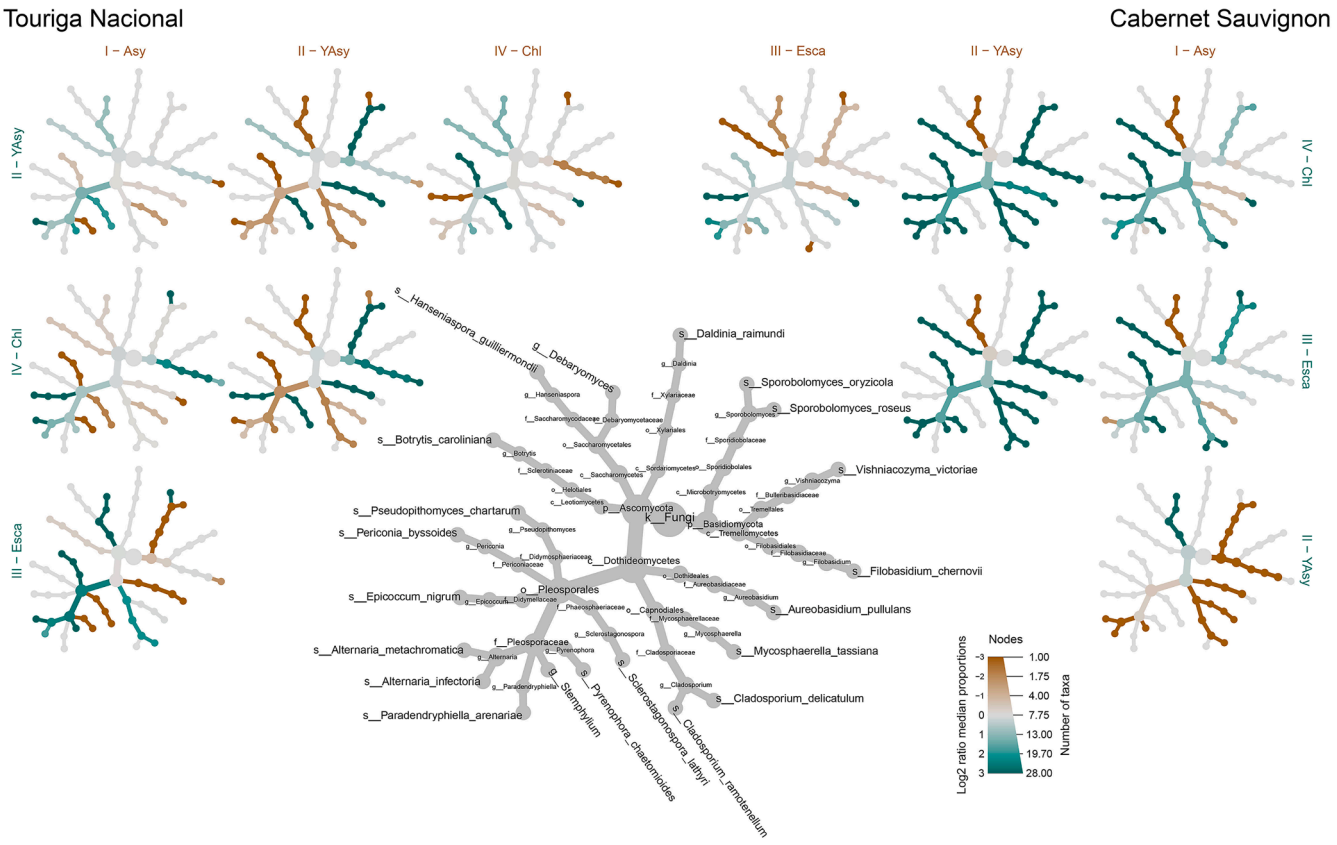

Fig. 4. Differential heat tree matrices depicting changes in fungal taxa abundance between leaf categories (Esca, Chl, Asy, YAsy) in grapevine cvs. Cabernet Sauvignon and Touring Nacional, in 2020, represented in the dataset, and in the grey cladogram, at a relative abundance (RA) > 0.1 %. The smaller cladograms show pairwise comparisons between each category, with the color illustrating the $\log_2$ fold change: a green node indicates a lower abundance of the taxon in the category on the abscissa than in the category on the ordinate. A brown node indicates the opposite.

3.4. Mycobiome and anthocyanins for different symptom phenotypes – objective 3

3.4.1. Mycobiome in different symptom phenotypes

3.4.1.1. Alpha diversity. The alpha diversity of the mycobiome does not vary when comparing cultivars, vintages, and symptom phenotypes ($P > 0.05$).

However, when looking at year/cultivar combinations, the Simpson and Inverted Simpson (InvSimpson) indices vary significantly among symptoms phenotypes (Fig. 5). In cv. Cabernet Sauvignon (2020), the Simpson index differs significantly when comparing Asy and Esca leaves ($P = 0.03$), and a trend is observed for the InvSimpson index ($P = 0.078$). However, in the same year, neither statistical differences nor trends are observed for cv. Touriga Nacional.

In Cabernet Sauvignon (2021), both Simpson and InvSimpson indices show trends of divergence when comparing BDA and Esca leaves ($P = 0.088$, $P = 0.096$). In the same year, in Touriga Nacional, both the Simpson and InvSimpson indices vary significantly when comparing BDA and Asy leaves ($P = 0.02$, $P = 0.019$) (Fig. 5).

3.4.1.2. Beta diversity. The beta diversity of the microbial composition varies significantly when comparing cultivars ($P = 0.006$) and vintages ($P = 0.001$), but not symptom phenotypes ($P > 0.05$).

When looking at year/cultivar combinations, the Bray–Curtis dissimilarity, represented in PCoA plots of the beta dispersion, varies significantly when comparing symptom phenotypes in Cabernet Sauvignon (2020, $P = 0.041$; 2021, $P = 0.001$), and Touriga Nacional (2021, $P = 0.007$), while a trend is found in Touriga Nacional (2020, $P = 0.08$) (Fig. 6).

In Cabernet Sauvignon (2020), the clustering pattern reveals that both Apox and Esca leaves have a trend of divergence from Asy leaves; in 2021, this trend is significant (Esca vs Asy; $P = 0.017$), along with a difference between Esca and BDA leaves ($P = 0.017$). In Touriga Nacional (2021), the post-hoc test show strong trends of divergence when comparing Esca and Asy leaves, as well as BDA and Asy leaves ($P = 0.085$). No differences in clustering are observed when comparing Asy and BDA leaves, in both cultivars and vintages.

3.4.1.3. Taxa abundance. The bar plots in Fig. 7 offer a visual representation of the 21 most abundant taxa detected in leaves of different symptom phenotypes and asymptomatic, in both cultivars and vintages.

When comparing symptom categories, in different years and cultivars, numerous taxa vary in abundance, as shown in Fig. 8. To find recurring patterns in taxa over- or under-representation when comparing symptom categories, we focus on those taxa that are similarly differently abundant either in the same cultivar in both years, or in the same year in both cultivars.

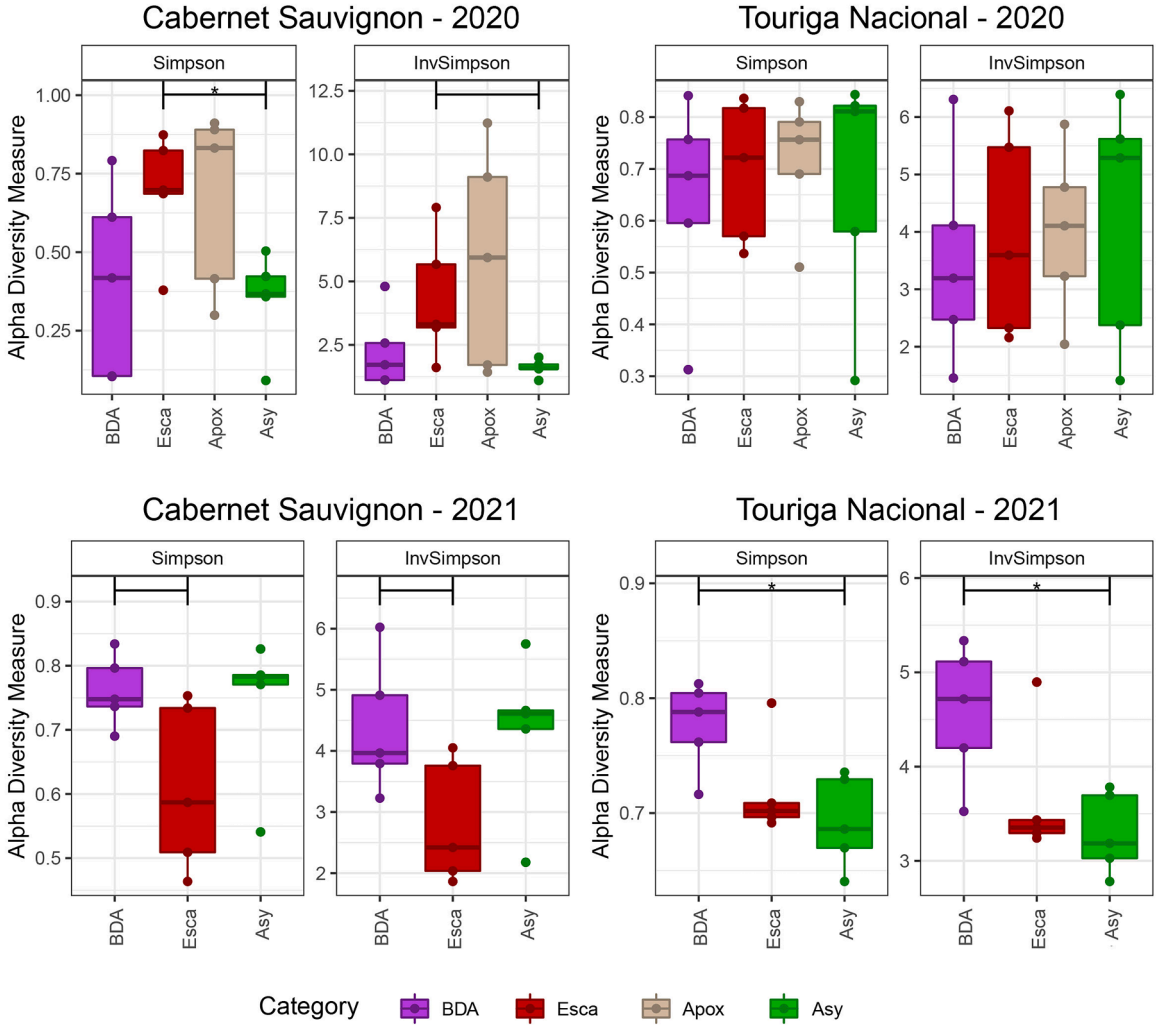

Fig. 5. Box plots of alpha diversity indices (Simpson and InvSimpson) showing the richness of the fungal communities in grapevine leaves under different symptom phenotypes (black dead arm [BDA], Esca, apoplectic [Apox]) and asymptomatic (Asy), in grapevine cvs. Cabernet Sauvignon and Touring Nacional, in 2020 and 2021. The horizontal brackets marked with an asterisk (*) indicate statistical differences, while brackets without asterisks indicate trends ($0.10 < P < 0.05$).

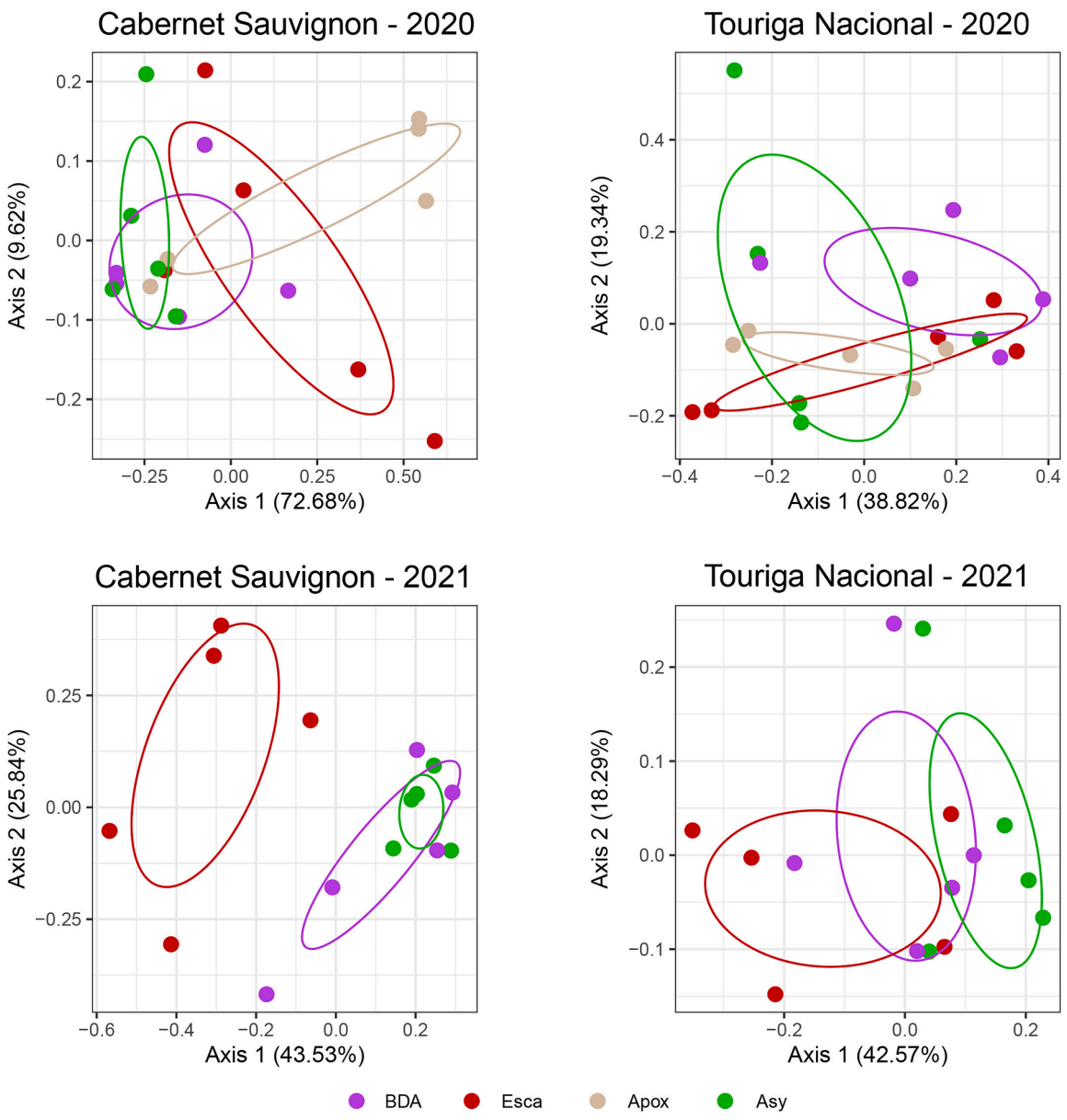

Fig. 6. PCoA plots of beta dispersion based on the Bray–Curtis dissimilarity of the fungal communities in grapevine leaves under different symptom phenotypes (black dead arm [BDA], Esca, apoplectic [Apox]) and asymptomatic (Asy), in grapevine cvs. Cabernet Sauvignon and Touring Nacional, in 2020 and 2021. Ellipses illustrate the multivariate normal distribution of samples within the same symptom category.

Esca* vs *Asy. In both vintages, *Botrytis caroliniana, Stemphylium* sp. and *Debaryomyces* sp. are consistently over-represented in Esca leaves, the first two taxa in Cabernet Sauvignon, the third in Touriga Nacional. *Stemphylium* sp. and *Daldinia raimundi* are two taxa over-represented in Esca leaves, in both cultivars, the former exclusively in 2020, the latter exclusively in 2021. On the other hand, *Epicoccum nigrum* and *Pseudopithomyces chartarum* are over-represented in Asy leaves, the former in both cultivars, only in 2021, the latter in both vintages, only in Touriga Nacional.

BDA* vs *Asy. No taxa are similarly over- or under-represented when comparing cultivars, in 2020, or vintages, in Cabernet Sauvignon. In both vintages, *Debaryomyces* sp. is over-represented in BDA leaves, while *P. chartarum* is more abundant in Asy leaves, exclusively in Touriga Nacional. In both cultivars, *Filobasidium* sp. and *D. raimundi* are over-represented in BDA leaves, while *E. nigrum* is more abundant in Asy leaves, only in 2021.

Esca* vs *BDA. In both vintages, *B. caroliniana, Stemphylium* sp., *Alternaria metachromatica* and *P. chartarum* are consistently over-represented in Esca leaves, the former two taxa in Cabernet Sauvignon, the latter two in Touriga Nacional. *P. chartarum, B. caroliniana and Paradendryphiella arenariae* are taxa over-represented in Esca leaves, in both cultivars, the former exclusively in 2020, the latter two exclusively in 2021. *Debaryomyces* sp., *Filobasidium* sp. and *Mycosphaerella tassiana* are over-represented in BDA leaves, either in both vintages, in a single cultivar, or in both cultivars, in a single year.

Apox* vs *Esca, BDA, Asy. When compared to all other categories, taxa over-represented in Apox leaves are *Filobasidium chernovii, Periconia byssoides* and *Vishniacozyma* sp., in Cabernet Sauvignon, and *Sporobolomyces oryzicola* and *E. nigrum*, in Touriga Nacional.

No taxon is exclusively present or consistently over- or under-represented in a specific symptom phenotype, in both vintages and cultivars.

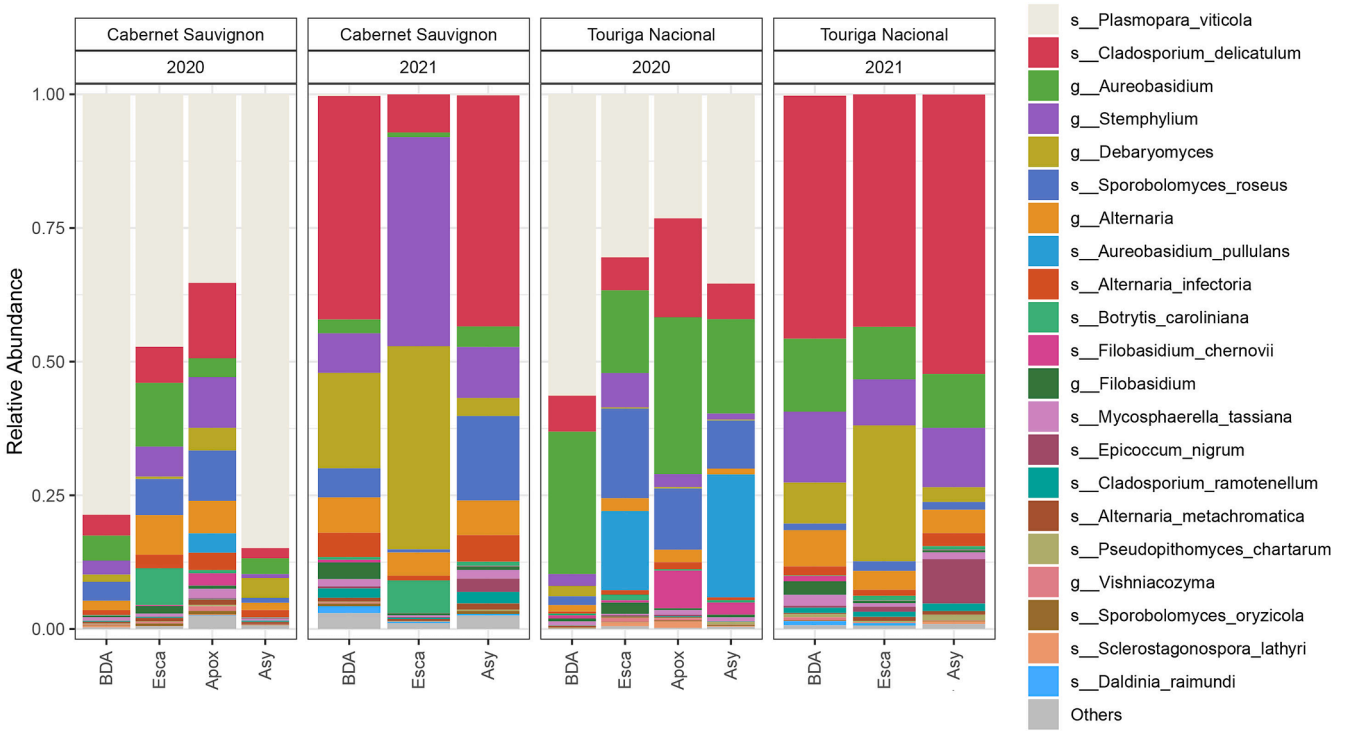

Fig. 7. Bar plots of the relative abundance of the 21 most abundant taxa identified at the genus (g_) or species (s_) level found in different symptom phenotypes (black dead arm [BDA], Esca, apoplectic [Apox]) and asymptomatic leaves (Asy), in grapevine cvs. Cabernet Sauvignon and Touriga Nacional, in 2020 and 2021. 'Others' are taxa not included among the 21 most abundant.

3.4.2. *Anthocyanins under different symptoms categories*

3.4.2.1. Total anthocyanins. In both vintages and cultivars, anthocyanins accumulated in Esca and BDA symptomatic leaves, while they were not detected in asymptomatic ones (Table 2). Regardless of symptom phenotype and vintage, total leaf anthocyanin concentration was always higher in Cabernet Sauvignon (452.2 - 724.4 mg kg^{-1}), when compared to Touriga Nacional (47.6 - 213.2 mg kg^{-1}). In Cabernet Sauvignon, the total anthocyanin concentration did not significantly differ when comparing Esca and BDA leaves, both in 2020 and 2021. Conversely, in Touriga Nacional, Esca leaves reached higher concentrations of total anthocyanins in both years, when compared to BDA (Table 2). In 2020, the total anthocyanin concentration depended on the factor 'cultivar' ($P \leq 0.0001$), and on the interaction 'cultivar*symptom phenotype' ($P \leq 0.001$), but not on 'symptom phenotype'. Instead, in 2021, significant differences were ascribable to 'cultivar' ($P \leq 0.0001$), to 'symptom phenotype' ($P \leq 0.001$), and to the interaction 'cultivar*symptom phenotype' ($P \leq 0.01$; Table 2).

3.4.2.2. Anthocyanin profile. The anthocyanin profile of Esca and BDA leaves highlights differences between the two cultivars and symptom phenotypes. The di-hydroxylated forms always displayed higher concentrations when compared to tri-hydroxylated and acyl-derivative anthocyanins, in both cultivars, symptom phenotypes, and vintages, with a prevalence of peonidin 3-*O*-glucoside, followed by cyanidin 3-*O*-glucoside, in most cases. This is especially evident in Touriga Nacional with BDA phenotype, where di-hydroxylated forms reached nearly 100 % of the total anthocyanin amount (Fig. 9). In 2020, significant differences in the accumulation of di-hydroxylated forms were ascribable to cultivar ($P \leq 0.0001$), symptom phenotype ($P \leq 0.01$), and the interaction cultivar*symptom phenotype ($P \leq 0.01$; Table 2). Instead, in 2021, the accumulation of di-hydroxylated anthocyanins was similar in Esca and BDA leaves within the same cultivar, but it differed significantly for cultivar ($P \leq 0.0001$), symptom phenotype ($P \leq 0.01$), and not for the interaction cultivar*symptom phenotype (Table 2). The concentration of tri-hydroxylated forms and acyl-derivatives was always higher in Esca leaves, regardless cultivar and vintage (Table 2). In 2020, tri-hydroxylated anthocyanins showed significant differences depending on symptom phenotype ($P \leq 0.0001$), and on the interaction cultivar*symptom phenotype ($P \leq 0.01$), but not on cultivar (Table 2), whereas in 2021, significant differences were also ascribable to cultivar ($P \leq 0.0001$; Table 2). The profile of tri-hydroxylated anthocyanins, regardless cultivar and symptom phenotype, showed malvidin 3-*O*-glucoside as the prevalent form, followed by petunidin and delphinidin 3-*O*-glucosides (Fig. 9). In 2020, acyl-derivatives showed highly significant differences depending on cultivar, symptom phenotype, and interaction cultivar*symptom phenotype ($P \leq 0.0001$); in 2021, highly significant differences were associated to cultivar ($P \leq 0.0001$) and symptom phenotype ($P \leq 0.01$), but not to the interaction cultivar*symptom phenotype.

3.4.3. *Correlation mycobiome - anthocyanins*

We analysed the relationship among fungal communities, single taxa and anthocyanins, both total and classes of different anthocyanin forms (di-hydroxylated, tri-hydroxylated, and acyl derivatives), using ordisurf plots (Fig. 10).

In 2021, the total anthocyanin levels significantly ($P = 0.017$) mapped onto the NMDS plot, revealing fungal species associated with varying anthocyanin concentrations. The value of anthocyanins at the location of each taxon-associated number, on each individual plot, indicates the anthocyanin concentration with which that taxon is associated, suggesting significant correlations. For example, *B. caroliniana, Stemphylium* and *Hanseniaspora guilliermondii* are more abundant in regions with high total anthocyanin concentrations, while *Filobasidium, Cladosporium ramotenellum* and *Aureobasidium* are associated with low concentrations. When examining classes of different anthocyanin forms (di-hydroxylated fit, $P = 0.038$; tri-hydroxylated fit, $P = 0.0085$; acyl derivates fit, $P = 9.34\ e^{-05}$), *B. caroliniana* and *Stemphylium* remain associated with the highest concentrations across all three classes, while

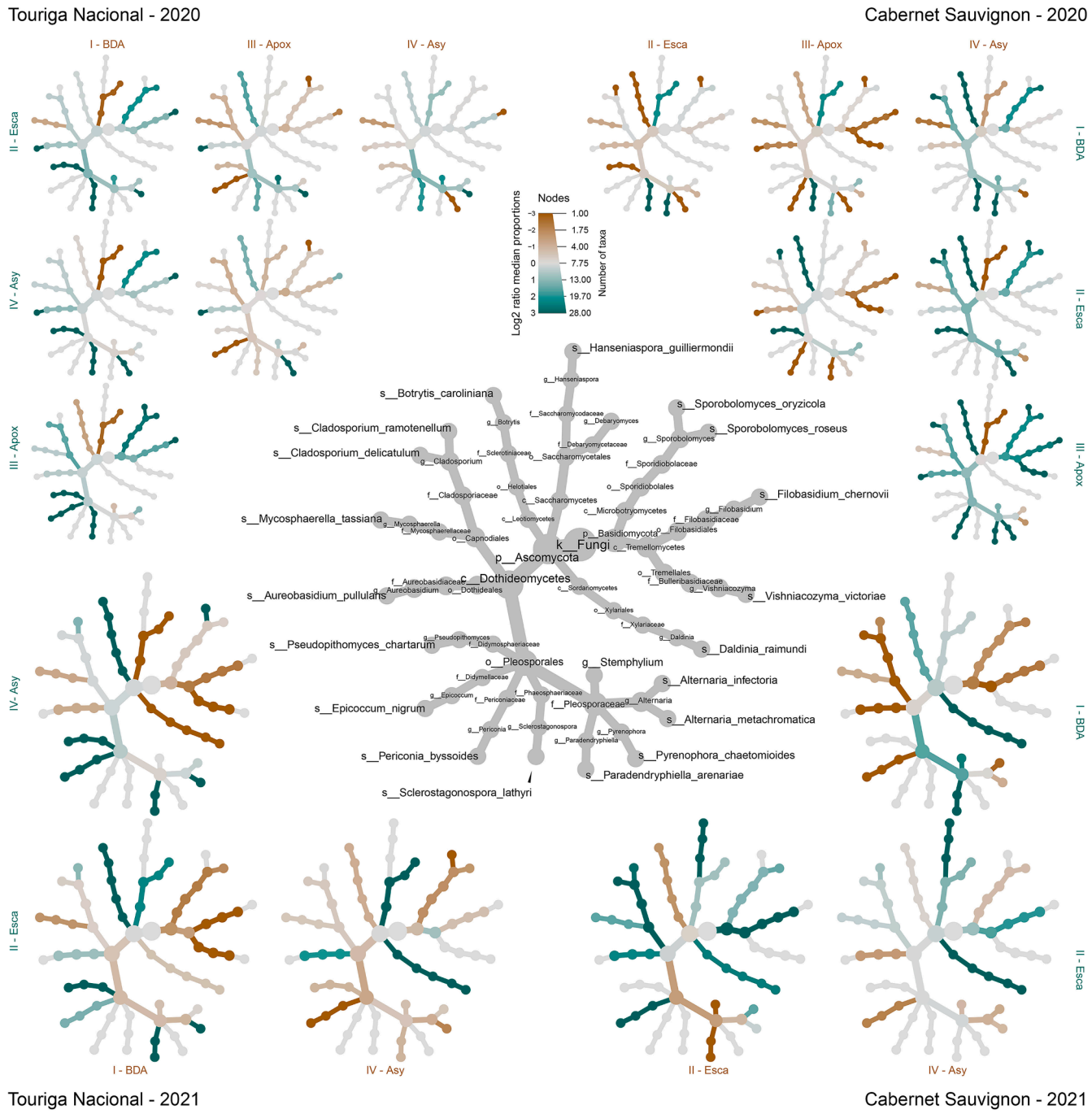

Fig. 8. Differential heat tree matrices depicting changes in fungal taxa abundance between leaf symptom phenotypes (black dead arm [BDA], Esca, apoplectic [Apox]) or asymptomatic (Asy), in grapevine cvs. Cabernet Sauvignon and Touring Nacional, in 2020 and 2021, represented in the dataset,and in the grey cladogram, at a relative abundance (RA) > 0.1 %. The smaller cladograms show pairwise comparisons between each symptom category, with the color illustrating the $\log_2$ fold change: a green node indicates a lower abundance of the taxon in the symptom category on the abscissa than in the symptom category on the ordinate. A brown node indicates the opposite.

H. guilliermondii is linked to high concentrations of di-hydroxylated anthocyanins and acyl derivatives, but only intermediate levels of tri-hydroxylated anthocyanins.

In Cabernet Sauvignon, the contour plots indicate higher anthocyanin concentrations in Esca leaves, with a clear separation of microbial species when compared to BDA leaves. In Touriga Nacional, samples are clustered on lower anthocyanin concentrations, and differences between Esca and BDA phenotypes are less clear.

In 2020, the dataset fit was found significant only for tri-hydroxylated anthocyanin ($P = 0.024$; Figure S1) and it is not further discussed.

4. Discussion

4.1. Endophytic mycobiome using NGS – objective 1

In recent years, numerous studies investigated the grapevine leaf microbiome, either employing whole leaves (i.e. endophytes and epiphytes) (Knapp et al., 2021; Liu and Howell, 2020; Pinto et al., 2014; Molnár et al., 2022; Kernaghan et al., 2017), or focusing on the leaf

Table 2
Total anthocyanin concentration (mg/kg dry weight) in Cabernet Sauvignon and Touriga Nacional leaves with different symptom phenotypes (Esca, black dead arm [BDA]) or asymptomatic (Asy), in 2020 and in 2021. Within each cultivar, mean values of total anthocyanins and class of different anthocyanin forms followed by different letters are significantly different for $P \leq 0.05$, according to a two-way ANOVA with a post hoc Bonferroni correction. Significant differences among cultivars, symptom phenotypes and their interactions were tested for $P \leq 0.01$ (*), $P \leq 0.001$ (**) and $P \leq 0.0001$ (***); ns = *not significant.*

2020	Symptom phenotype	Di-hydroxylated (mg/kg)	Tri-hydroxylated (mg/kg)	Acyl-derivatives (mg/kg)	Total anthocyanins (mg/kg)
Cabernet Sauvignon					
	Esca	214.2 ± 26.5 b	68.9 ± 6.7 a	169.1 ± 17.4 a	452.2 ± 34.7 a
	BDA	549.0 ± 85.4 a	18.0 ± 2.3 ab	94.0 ± 12.3 ab	661.0 ± 83.6 a
	Asy	0.0	0.0	0.0	0.0
Touriga Nacional					
	Esca	92.2 ± 6.8 c	78.9 ± 1.6 a	42.1 ± 12.2 b	213.2 ± 16.4 b
	BDA	96.8 ± 10.8 c	4.1 ± 3.3 b	0.02 ± 0.01 c	100.9 ± 11.1 c
	Asy	0.0	0.0	0.0	0.0
Cultivar		***	ns	***	***
Symptom phenotype		*	***	***	ns
Cultivar*Symptom phenotype		*	*	***	**

2021	Symptom phenotype	Di-hydroxylated (mg/kg)	Tri-hydroxylated (mg/kg)	Acyl-derivatives (mg/kg)	Total Anthocyanins (mg/kg)
Cabernet Sauvignon					
	Esca	483.7 ± 15.0 a	83.9 ± 9.7 a	156.8 ± 7.3 a	724.4 ± 4.9 a
	BDA	422.0 ± 88.1 a	36.7 ± 6.5 b	91.1 ± 15.0 a	549.8 ± 109.3 a
	Asy	0.0	0.0	0.0	0.0
Touriga Nacional					
	Esca	85.0 ± 3.7 b	39.9 ± 1.8 b	12.2 ± 5.3 b	137.1 ± 6.9 b
	BDA	47.6 ± 9.5 b	0.01 ± 0.01 c	0.01 ± 0.01 c	47.6 ± 9.5 c
	Asy	0.0	0.0	0.0	0.0
Cultivar		***	***	***	***
Symptom phenotype		*	***	*	**
Cultivar*Symptom phenotype		Ns	***	ns	*

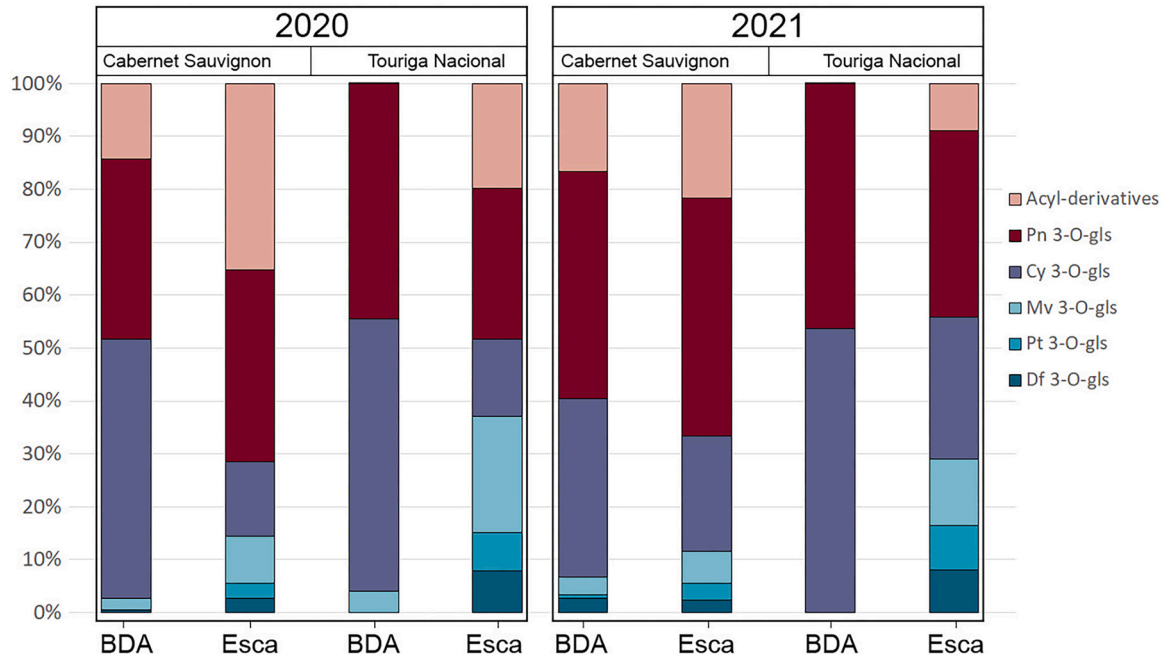

Fig. 9. Anthocyanin profile (%) of Cabernet Sauvignon (CS) and Touriga Nacional (TN) leaves under Esca or black dead arm (BDA) phenotypes, in 2020 and 2021. Mv 3-*O*-gls = malvidin 3-O-glucoside; Pn 3-*O*-gls = peonidin 3-*O*-glucoside; Pt 3-*O*-gls = petunidin 3-*O*-glucoside; Cy 3-*O*-gls = cyanidin 3-*O*-glucoside; Df 3-*O*-gls= delphinidin 3-*O*-glucoside and sum of acylated forms (acyl-derivatives).

phyllosphere (Singh et al., 2018a; Singh et al., 2018b; Gobbi et al., 2020; Papadopoulou et al., 2022). To our knowledge, only three studies looked exclusively into the *Vitis* spp. leaf endophytic mycobiome (Fan et al., 2020; Aleynova et al., 2022; Aleynova et al., 2023), using NGS techniques.

When compared to the fungal communities found in whole leaves or phyllosphere, leaf endophytes are believed to contribute to a smaller extent to the total species richness (Behrens and Fischer, 2022). Our results are in line with those obtained in a previous study (Fan et al., 2020), where the authors detected 150 fungal genera in V. *vinifera* and

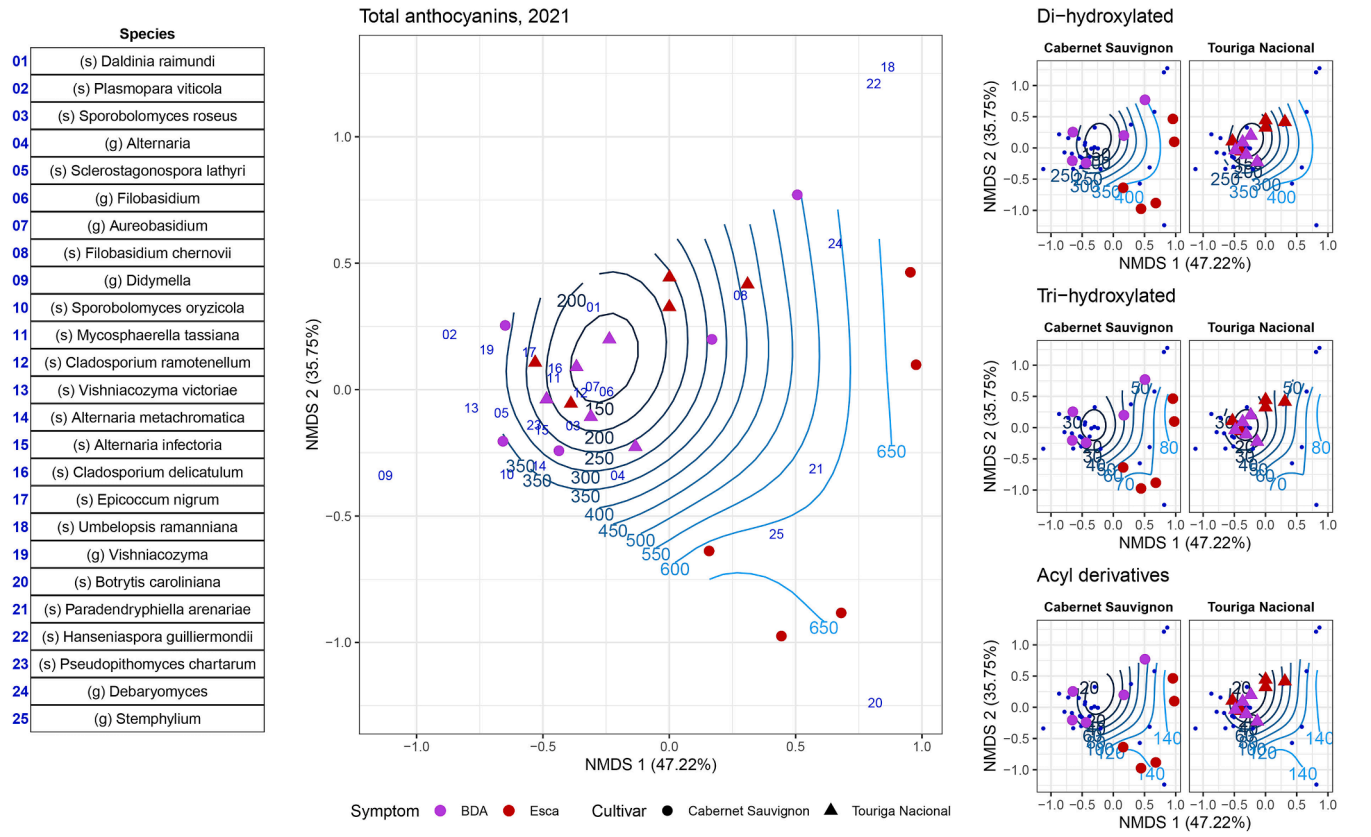

Fig. 10. Non-metric multidimensional scaling plots representing microbial and anthocyanin data for year 2021. Microbiome samples are plotted as large dots (circles and triangles) while single fungal taxa (RA>0.1 %) are represented as blue numbers in the "Total Anthocyanins" plot and corresponding species list (leftmost panel). Contours indicate anthocyanin concentration gradients. Three sets of plots display di-hydroxylated, tri-hydroxylated, and acyl derivative anthocyanin profiles, separated by grapevine cultivar. In these plots, species are represented by small blue dots, and contours show variations in specific anthocyanin levels.

V. *amurensis* leaves (162 genera in the present study), but considerably greater than what was reported a couple of years before by Aleynova and colleagues, in V. *amurensis* (64 genera) (Aleynova et al., 2022), and later in other *Vitis* spp. hybrids (62 to 87 genera) (Aleynova et al., 2023). Excluding *Plasmopara viticola*, whose presence in 2020 was due to improper timing in the application of plant protection products, brought about by Covid-related restrictions, numerous abundant taxa found in our study, such as *Cladosporium* spp., *Alternaria* spp., *Aureobasidium, Mycosphaerella* and *Filobasidium*, have been previously reported in the grapevine endosphere (Aleynova et al., 2022; Aleynova et al., 2023) and in other studies that analyzed whole leaves or phyllosphere (Knapp et al., 2021; Liu and Howell, 2020; Singh et al., 2018b; Gobbi et al., 2020; Papadopoulou et al., 2022; Barroso-Bergadà et al., 2023). Surprisingly, only few abundant taxa (RA>1 %), e.g. *Cladosporium*, are shared between our study and that of Fan and colleagues (Fan et al., 2020), in *Vitis* spp., suggesting large genotype- or environmental-driven variability in microbial composition.

Interestingly, *P. viticola* was detected in high abundances (in 2020) despite leaves being free of visible lesions produced by this oomycete. A similar observation was recently reported (Aleynova et al., 2023), highlighting a lag period between pathogen infection, tissue colonization and symptoms manifestation. GTD-associated fungi were not expected in leaves (Mugnai et al., 1999), and our data confirms that they do not constitute a sizable component of the endophytic mycobiome. However, the detection of small abundances (RA<0.01 %) of *Diplodia, Phaeomoniella chlamydospora, Fomitiporia* and *Neofusicoccum* suggests that their genetic material may find its way to leaves.

When looking at whole leaves or leaf phyllosphere, cultivar-dependent differences in mycobiome composition, either in terms of community indices or individual taxa abundance, are reported in multiple studies (Molnár et al., 2022; Singh et al., 2018a; Singh et al., 2018B; Papadopoulou et al., 2022). Concerning leaf endophytes, (Fan et al., 2020; Aleynova et al., 2023) detected significant differences when comparing *Vitis* species or hybrids, however, in literature, there are no reports over the cultivar effect on the mycobiome composition of V. *vinifera*, using culture-independent approaches. In this study, we reveal, for the first time in the leaf endosphere, differences in taxa composition, abundance and beta diversity between Cabernet Sauvignon and Touriga Nacional.

Vintage is a strong predictor of fungal community diversity at the phyllosphere level (Knapp et al., 2021; Papadopoulou et al., 2022). This is suggested to be due to multiple factors, one of the most mentioned being meteorological conditions. In our study, vintage is a highly significant factor in predicting community diversity; however, the infection by *P. viticola* (year 2020) seems the main driver of observed differences (Barroso-Bergadà et al., 2023).

4.2. *Mycobiome during symptoms progression in Esca leaves – objective 2*

To explore microbial dynamics during esca symptom progression, from the scattered chlorotic spots stage (Chl) to fully symptomatic leaves (Esca; Fig. 1A-D), we compared the mycobiome profile of symptomatic and asymptomatic leaves of different ages, in Cabernet Sauvignon and Touriga Nacional, in 2020. We focus the following discussion on two key observations.

First, the mycobiome beta diversity of Chl leaves differs from that of asymptomatic leaves of the same age (YAsy), along with several taxa over- or under-represented, in both cultivars (Fig. 4). This suggests that the physiological/biochemical events that lead to the appearance of chlorotic spots alter the abundance of fungal endophytes in leaves,

favoring certain taxa (e.g. *Aureobasidium* sp., *E. nigrum*) over others (*Debaryomyces* sp.). Second, the mycobiome profile of Chl and Esca leaves does not differ for any measured index, and only few taxa are over- or under-represented (e.g. *B. caroliniana, E. nigrum*). These observations suggest that the mycobiome composition is mostly shaped during the early stages of symptom development, and only a small number of taxa are influenced by subsequent events, such as the appearance of pigmentation typical of Esca leaves (Fig. 4, Table 2). We find reasonable to hypothesize that community alterations may occur even before the appearance of chlorotic spots, along with physiological alterations that are known to precede symptoms expression (Magnin-robert et al., 2017; Valtaud et al., 2011; Goufo and Cortez, 2020; Magnin-Robert et al., 2011; Calamai et al., 2014; Christen et al., 2007; Goufo and Cortez, 2023). From this perspective, fungal communities may be passive spectators that adapt to environmental circumstances, or they may be actively involved in the events that lead to (or prevent) symptoms onset. For example, certain fungi may negatively affect plant physiology or gene expression, as suggested by the activation of plant defenses in pre-symptomatic leaves (Magnin-Robert et al., 2011), or they may positively affect leaves -that remain asymptomatic- by detoxifying putative leaf symptoms-inducing molecules (Del Frari et al., 2022; Giauque et al., 2019). The fungi over-represented in Chl leaves, when compared to YAsy leaves (Fig. 4), i.e. *S. roseus, E. nigrum, Aureobasidium* sp. and *Filobasidium* sp., are not known grapevine pathogens, despite *A. pullulans* abundance in grapevine wood being recently associated to increased severity of Esca tiger stripes (Karácsony et al., 2023). These, and other, fungi may even alter their lifestyle in response to leaf senescence-like processes, that are reported during early symptoms development (Bortolami et al., 2023). On the other hand, *Debaryomyces*, a genus involved in the biological control of several plant pathogens (Hernandez-Montiel et al., 2018; Medina-Córdova et al., 2018; Droby et al., Aug. 1989), and whose role in the grapevine endosphere remains unknown, is abundant in YAsy leaves but absent in Chl leaves, in both cultivars (Fig. 4). This genus may be especially sensitive to the plant physiological changes that precede symptoms onset, and its temporary absence may -hypothetically- deprive the plant of a beneficial taxon useful to maintain community homeostasis or involved in detoxification.

4.3. Symptoms phenotypes: mycobiome and anthocyanins – objective 3

In this study, we present the first microbiological evaluation of grapevine leaves affected by interveinal necrosis and manifesting different symptom phenotypes, as well as their qualitative and quantitative anthocyanin composition. In previous studies, other authors demonstrated that endophytes can manipulate their host, leading to alterations in their metabolite profile, including that of anthocyanins (Yu et al., 2020), therefore, we aimed at understanding whether there is a correlation between leaf mycobiome and anthocyanins.

There are numerous factors that contribute to shaping microbial composition and anthocyanin amounts and profiles, complicating the establishment of a direct correlation. Two well-known factors are grapevine genotype and vintage (Papadopoulou et al., 2022; Aleynova et al., 2023); a third is sampling time, and a fourth is the inherent phenotypic variability observed in each individual leaf. Sampling timing is a critical factor for three main reasons. (i) A pathogen attack, such as the one observed in 2020 for *P. viticola*, may rapidly alter microbial and metabolic profiles (Barroso-Bergadà et al., 2023; Nascimento et al., 2019), affecting genotypes differently, depending on their susceptibility to this oomycete. (ii) The application of plant protection products, which typically precedes symptom onset, likely alters leaf microbial composition (Gobbi et al., 2020; Rantsiou et al., 2020; Sumby et al., 2021), leading to an over- or under-representation of certain taxa in the sequence of events preceding symptom development. (iii) The anthocyanin profile may vary rapidly depending on the symptom 'stage,' as suggested in a preliminary study (Larignon et al., 2004). Regarding phenotypic variability, we based our sampling on the percentage of necrotic tissue, *i.e.*, 10–25 % of the total leaf area; however, there is also variability in the area of pigmented leaf blade, when comparing individual leaves. Some exhibit approximately a 50:50 ratio of pigmented-green tissue (Fig. 1, I), while others have less pigmented area, *e.g.*, 20:80. This may influence both anthocyanin measurements and fungal abundance, as certain fungi may preferentially colonize pigmented tissue. Future studies should keep in consideration these factors to refine our understanding of specific aspects of esca leaf stripe symptom.

Despite these challenges, our results reveal major differences in microbial composition and anthocyanin profiles between symptomatic and asymptomatic leaves, as well as among different symptom phenotypes.

4.3.1. Mycobiome

The symptom phenotypes under examination and asymptomatic leaves often differ in terms of community indices and individual taxa abundance, though this is cultivar- and/or vintage-dependent. When examining community indices, significant differences or strong trends are observed when comparing Esca and Asy leaves in Cabernet Sauvignon. This highlights the major alterations occurring in the fungal community profile during Esca symptom development, as described earlier. Trends are also observed in Touriga Nacional, although not across both examined years (Figs. 5 and 6). *Botrytis caroliniana* and *Stemphylium* sp. are often over-represented (or exclusively present) in Esca leaves, particularly in Cabernet Sauvignon, where an over-representation of *Botrytis* sp. in red-colored leaves was previously reported (Chen et al., 2020), supporting our findings. It remains to be determined whether *B. caroliniana* colonizes exclusively red-pigmented tissue or the entire leaf (both pigmented and green tissues) and to evaluate whether this taxon engages in host manipulation or finds a preferential niche in leaves undergoing physiological alterations that lead to the development of red pigmentation.

On the other hand, neither BDA nor Apox leaves differ from Asy leaves in any community index across both vintages and cultivars, with only one exception (Fig. 5). In this case, the sequence of events leading to these symptom phenotypes did not significantly affect fungal communities, and individual taxa are only moderately affected (Fig. 8). Notably, none of the taxa over-represented in purple leaves in (Chen et al., 2020) are similarly over-represented in BDA leaves in our study.

Examining community indices, Esca and BDA leaves differ significantly in one cultivar/vintage combination (beta diversity in Cabernet Sauvignon – 2021), although multiple trends are observed. Among the several taxa over- or under-represented in each symptom phenotype (Fig. 8), *B. caroliniana* is significantly more abundant (or exclusively present) in Esca leaves, further emphasizing this fungus involvement in this symptom phenotype.

Overall, this suggests that, among the 'Esca – BDA – Asy' leaves, BDA leaves occupy an intermediate position, as their endophytic fungal communities differ moderately from both Esca and Asy leaves (Fig. 6).

It is difficult to identify a clear pattern that suggests a strong involvement of microbial structures or specific taxa in the Apox symptom phenotype, since the evaluation was conducted for only one year. It is possible that the rapid sequence of events leading to symptom onset and eventual leaf fall occurs so quickly that fungal endophytes have a very limited time to respond (Magnin-robert et al., 2016).

4.3.2. Anthocyanins

In this study, in both cultivars, Esca and BDA leaves accumulated significant amounts of anthocyanins, while no anthocyanins were detected in Asy leaves. The absence -or the presence of trace amounts- of anthocyanins in healthy and non-senescing leaves has been previously demonstrated in V. *vinifera* (Kedrina-okutan et al., 2018; Negro et al., 2020; Gutha et al., 2010; Guidoni et al., 1997).

The total anthocyanin accumulation in Cabernet Sauvignon leaves was higher than in Touriga Nacional, in both vintages, regardless of the symptom phenotype. This confirms that the ability to accumulate

anthocyanins in vegetative organs (beyond berries) is a cultivar-specific trait. Touriga Nacional accumulated more anthocyanins in Esca leaves compared to BDA leaves, highlighting that, in this cultivar, anthocyanin accumulation also depends on the interaction cultivar*symptom phenotype (Table 2).

Unlike berries, few studies have explored the anthocyanin profile of grapevine leaves. It is known that grapevine leaves mainly accumulate cyanidin-based anthocyanins and, to a lesser extent, tri-hydroxylated forms, as the expression of flavonoid 3′5′ hydroxylase in grapevine leaves is limited (Kobayashi et al., 2009). For example, Pinot Noir leaves accumulate di-hydroxylated anthocyanins (Matus et al., 2017), and cyanidin 3-*O*-glucoside is the prevalent form in Sangiovese leaves (Negro et al., 2020). Similarly, in Yan73 leaves, over 40 % of total anthocyanins were peonidin-derivatives, followed by cyanidin-derivatives (20 %) (Xie et al., 2020; Guan et al., 2012). In the present study, di-hydroxylated anthocyanins made up 69 % of the total concentration in Cabernet Sauvignon and 75 % in Touriga Nacional, consistent with findings in other varieties (Fig. 9). Unlike leaves, tri-hydroxylation in berries is generally prevalent relative to di-hydroxylation (Ferrandino et al., 2012), and acylation, besides being genotype–dependent, is largely a response to stress conditions, for example high temperatures and limited water availability. Besides, in berries, acylation of free anthocyanins happens later relative to the formation of the free forms, increasing thermostability.

Both Cabernet Sauvignon and Touriga Nacional primarily accumulated di-hydroxylated anthocyanins, with the highest levels observed in Touriga Nacional BDA phenotype (2021), where they accounted for 100 % of the total anthocyanin concentration. Since methylation occurs after the formation of the simplest non-methylated di-hydroxylated anthocyanin (i.e. cyanidin 3-*O*-glucoside), the BDA phenotype may represent an early stage of symptom development, which could either progress to the Esca phenotype or remain as BDA (Lecomte et al., 2012). This transition may trigger the methylation of the initial non-methylated anthocyanins. This is likely associated with BDA pigmentation (Fig. 1, I), wine-red to dark purple, with an average cyanidin 3-O-glucoside incidence of 50 % of the total amount. If the leaves alter to Esca pigmentation, dominated by forms with higher levels of methylation (peonidin 3-*O*-glucoside and the tri-hydroxylated malvidin 3-*O*-glucoside), the color shifts to tonalities of red (Fig. 1, II). This is especially relevant in Touriga Nacional, where tri-hydroxylated anthocyanins and acyl-derivatives accumulated in Esca leaves but were absent or only present in trace amounts in BDA leaves. In Cabernet Sauvignon, tri-hydroxylated anthocyanins and acyl-derivatives were detected in both symptom phenotypes, however, always in lower amounts in BDA leaves.

The higher level of acylation found in the combination grapevine*Esca leaves, regardless the cultivar, could be considered as a specific response of grapevine leaf tissue to esca, in line with what happens in berries, where acylation happens later relative to the formation of the simplest non-acylated free forms. Thus, through the analysis of the anthocyanin profile of symptomatic leaves, we can support the hypothesis of the transition from BDA infection, resulting in the prevalent accumulation of the simplest cyanidin 3-*O*-glucoside, to the esca syndrome. This development, particularly in Cabernet Sauvignon leaves, resulted in a high total anthocyanin concentration, a high incidence of tri-hydroxylated and acylated anthocyanins (average of the two seasons 41.5 % over total amounts), respect to BDA-affected leaves where their average percentage incidence stopped at 20 % (Fig. 9).

4.3.3. *Mycobiome and anthocyanins*

When comparing the Esca and BDA phenotypes, the differences observed both in mycobiome and anthocyanin profiles suggests a strong correlation between the two (Fig. 10).

Our result show that there is no single taxon exclusively present or significantly over-represented only in Esca or only in BDA leaves, across cultivars and vintages. This is not in support of the hypothesis that fungi are responsible for manipulating their host toward the accumulation of anthocyanins (Collinge et al., 2022; Pan et al., 2020; Yu et al., 2020), leading to either symptom phenotype, even though the role of *B. caroliniana* should be further explored. Instead, we hypothesize that physiological and biochemical events that occur in leaves lead to alterations in fungal endophytes abundance. In this scenario, taxa under- or over-represented in specific symptom phenotypes suggest different tolerance to such events. These include alterations in hormonal and lipidic profiles (Goufo and Cortez, 2020), phytoalexins accumulation (Calzarano et al., 2016), the synthesis of anthocyanins precursors, such as p-coumaric acid and quercetin, molecules with known antifungal activity (Hu et al., 2023; Nguyen and Bhattacharya, 2022), and the expression of defense-related genes (*e.g.* chitinases and other PR-proteins) (Valtaud et al., 2009; Magnin-Robert et al., 2011).

The microbial structure and lack of anthocyanin accumulation in Asy leaves are altered when examining BDA leaves. Here, we observe mild changes in microbial composition and the exclusive accumulation of di-hydroxylated anthocyanins in Touriga Nacional, with moderate amounts of tri-hydroxylated anthocyanins and acyl derivatives in Cabernet Sauvignon (Figs. 6 and 9). This indicates a BDA-specific triggering factor, occurring earlier in the season, leading to minor or no cytological and histological changes in affected leaves and canes (Valtaud et al., 2011; Fleurat-Lessard et al., 2013). In contrast, Esca leaves show more pronounced microbial alterations, accompanied by a greater accumulation of tri-hydroxylated anthocyanins and acyl derivatives in both cultivars, both associated with stronger stress responses (Figs. 6 and 9). This suggests an Esca-specific triggering factor, occurring slightly later in the season, leading to major cytological and histological changes in affected tissues (Valtaud et al., 2011; Fleurat-Lessard et al., 2013).

Alternatively, a single triggering factor could regulate the expression of either BDA or Esca phenotypes in a concentration-dependent manner, with low concentrations leading to BDA and high concentrations resulting in Esca.

Overall, the evidence and insights presented in this study support the view that the BDA and Esca leaf phenotypes are distinct. We can speculate that intermediate phenotypes, or the transition from BDA to Esca (and never *vice versa*), may result from the simultaneous or sequential action of the Esca and BDA triggering factors. This hypothesis does not deal with the origin of the triggering factors, therefore, Larignon's original view that the BDA phenotype has different etiological agents from Esca remains to be verified (Larignon et al., 2009). The present study, however, highlights the need to identify the triggering factor(s) to move a step forward.

On this matter, it has been demonstrated that during esca progression in woody tissues, besides the reduction of the sapwood functionality (Gómez et al., 2016), there may be impairments also in the sap flow of the leaves. This leads to a vascular occlusion and cavitation phenomena (Bortolami et al., 2023; Bortolami et al., 2019) which could affect the leaf xylemic vessels and, probably, bring about disruptions of phloem transport, involving, to some extent, the regular translocation of nutrients, especially sugars. The impairment in sugar transport out of the leaf can trigger sugar accumulation, and consequently, anthocyanin accumulation. It is well and longtime known (Pirie and Mullins, 1976) that carbohydrate accumulation induces the up-regulation of the phenylpropanoid pathway, notably increasing the anthocyanin accumulation (Weiss, 2000; Teng et al., 2005; Solfanelli et al., 2006; Murakami et al., 2008; Peng et al., 2008). However, sugar increase is not the only driver of anthocyanin accumulation; in fact, the berry anthocyanin accumulation involves a synergic effect between sugar accumulation and abscisic acid (Pirie and Mullins, 1976), a key-mediator of stress (Ferrandino and Lovisolo, 2014; Cao et al., 2011), and a senescence-related hormone (Pirie and Mullins, 1976; Gao et al., 2016; Zhao et al., 2016). It was previously demonstrated that carbohydrate metabolism is altered in Esca leaves, with an accumulation of fructose (Valtaud et al., 2011). Additionally, there is an increased abundance of

senescence-related hormones, such as abscisic acid, jasmonic acid, and salicylic acid, when compared to asymptomatic leaves (Goufo and Cortez, 2020). The accumulation of anthocyanins, along with the presence of senescence-related hormones and vascular occlusions, shares several similarities with leaf senescence processes, as previously suggested by (Bortolami et al., 2023).

5. Conclusion

This study provides new insights into the interplay between fungal communities and anthocyanin profiles in grapevine leaves affected by esca and related symptom phenotypes. Using DNA metabarcoding, we observed that Esca symptom progression correlates with shifts in fungal diversity, suggesting early biochemical events that precede the appearance red pigmentation. In addition, our findings highlight significant differences in fungal composition and anthocyanin profiles across symptom phenotypes, with *Botrytis caroliniana* being especially associated with red pigmentation. While di-hydroxylated anthocyanins dominated in BDA leaves, tri-hydroxylated anthocyanins accumulated more in Esca leaves, suggesting a potential progression between these phenotypes driven by biochemical and microbial changes. No single fungal taxon was uniquely linked to a specific symptom phenotype, indicating that microbial shifts likely respond to, rather than trigger, host physiological and biochemical alterations. Anthocyanins emerged as both stress-response metabolites and potential indicators of disease progression.

Future studies should investigate the molecular interactions between fungal communities and host metabolism to better understand the mechanisms driving these changes. Additionally, exploring the genetic and environmental factors influencing symptom variability could aid in developing strategies to mitigate trunk diseases impact and improve vineyard sustainability.

Funding

This work was funded by Portuguese national funds through FCT – Fundação para a Ciência e a Tecnologia, I.P., under the projects: UIDB/04129/2020 of LEAF-Linking Landscape, Environment, Agriculture and Food, Research Unit; SuberPhyto (02/SAICT/2017). A.C. was funded by Portuguese national funds (OE), through FCT, I.P., in the scope of the framework contract foreseen in numbers 4–6 of article-23, of the Decree-Law 57/2016, 29 August, changed by Law 57/2017, 19 July (DL 57/2016/CP1382/CT0010). This work was partly supported and funded by: the Novo Nordisk Foundation with grant number NNF19SA0059348 (The MATRIX), for A.G. and L.H.H.; Fondo Ricerca locale 2022 delivered by the University of Turin, for C.I. and A.F.

CRediT authorship contribution statement

Giovanni Del Frari: Writing – review & editing, Writing – original draft, Visualization, Investigation, Funding acquisition, Conceptualization. **Chiara Ingrà:** Writing – original draft, Visualization, Investigation, Formal analysis, Data curation. **Marie Rønne Aggerbeck:** Writing – review & editing, Writing – original draft, Visualization, Formal analysis, Data curation. **Alex Gobbi:** Investigation, Data curation. **Teresa Nascimento:** Investigation. **Ana Cabral:** Investigation. **Helena Oliveira:** Writing – review & editing, Funding acquisition. **Lars Hestbjerg Hansen:** Writing – review & editing, Funding acquisition. **Alessandra Ferrandino:** Writing – review & editing, Writing – original draft, Supervision, Funding acquisition. **Ricardo Boavida Ferreira:** Writing – review & editing, Supervision, Funding acquisition.

Declaration of competing interest

The authors declare that they have no known competing financial interests or personal relationships that could have appeared to influence the work reported in this paper.

Acknowledgements

The authors would like to acknowledge Valeria Cascavilla, Lorenzo Volpi and Madalena Gracio for assistance during field sampling and/or wet-lab work.

Supplementary materials

Supplementary material associated with this article can be found, in the online version, at doi:10.1016/j.stress.2025.100793.

Data availability

Sequencing data is publicly available - see manuscript

References

Aleynova, O.A., et al., 2023. Bacterial and fungal endophytes of grapevine cultivars growing in Primorsky Krai of Russia. Horticulturae 9 (12), 1–18. https://doi.org/10.3390/horticulturae9121257, 1257.

Aleynova, O.A., Nityagovsky, N.N., Suprun, A.R., Ananev, A.A., Dubrovina, A.S., Kiselev, K.V., Oct. 2022. The diversity of fungal endophytes from wild grape *Vitis amurensis* Rupr. Plants 11 (21), 2897. https://doi.org/10.3390/plants11212897.

P.Martinez Arbizu, "pairwiseAdonis: pairwise multilevel comparison using adonis", *R package version 0.4*. p. 1, 2020.

Barroso-Bergadà, D., et al., 2023. Leaf microbiome data for european cultivated grapevine (*Vitis vinifera*) during downy mildew (*Plasmopara viticola*) epidemics in three wine-producing regions in France. PhytoFrontiers 3 (2), 477–483. https://doi.org/10.1094/PHYTOFR-11-22-0138-A.

Behrens, F.H., Fischer, M., 2022. Evaluation of different phyllosphere sample types for parallel metabarcoding of fungi and oomycetes in *Vitis vinifera*. Phytobiomes. J. 6 (3), 207–213. https://doi.org/10.1094/pbiomes-11-21-0072-sc.

Bokulich, N.A., et al., 2018. Optimizing taxonomic classification of marker-gene amplicon sequences with QIIME 2's q2-feature-classifier plugin. Microbiome 6 (1), 1–17. https://doi.org/10.1186/s40168-018-0470-z.

Bortolami, G., et al., 2019. Exploring the hydraulic failure hypothesis of esca leaf symptom formation. Plant Physiol. 181 (November), 1163–1174. https://doi.org/10.1104/pp.19.00591.

Bortolami, G., et al., Mar. 2023. Esca grapevine disease involves leaf hydraulic failure and represents a unique premature senescence process. Tree Physiol. 43 (3), 441–451. https://doi.org/10.1093/treephys/tpac133.

Calamai, L., Goretti, A., Surico, G., Mugnai, L., 2014. Grapevine leaf stripe disease: a metabolomic approach by GC–MS identifies affected vines before symptom appearance. Phytopathol. Mediterr. 53, 580. https://doi.org/10.14601/Phytopathol_Mediterr-15167.

Callahan, B.J., McMurdie, P.J., Holmes, S.P., 2017. Exact sequence variants should replace operational taxonomic units in marker-gene data analysis. ISME J. 11 (12), 2639–2643. https://doi.org/10.1038/ismej.2017.119.

Calzarano, F., et al., 2016. Patterns of phytoalexins in the grapevine leaf stripe disease (esca complex)/grapevine pathosystem. Phytopathol. Mediterr. 55 (3), 410–426. https://doi.org/10.14601/Phytopathol_Mediterr-18681.

Calzarano, F., et al., 2021. Factors involved on tiger-stripe foliar symptom expression of esca of grapevine. Plants 10 (1041). https://doi.org/10.3390/plants10061041.

Cao, F.Y., Yoshioka, K., Desveaux, D., 2011. The roles of ABA in plant-pathogen interactions. J. Plant Res. 124 (4), 489–499. https://doi.org/10.1007/s10265-011-0409-y.

Caporaso, J.G., et al., 2010. QIIME allows analysis of high-throughput community sequencing data. Nat. Methods 7 (5), 335–336. https://doi.org/10.1038/nmeth.f.303.

Castellarin, S.D., Di Gaspero, G., 2007. Transcriptional control of anthocyanin biosynthetic genes in extreme phenotypes for berry pigmentation of naturally occurring grapevines. BMC Plant Biol. 7, 46. https://doi.org/10.1186/1471-2229-7-46.

Castellarin, S.D., Di Gaspero, G., Marconi, R., et al., 2006. Colour variation in red grapevines (*Vitis vinifera* L.): genomic organisation, expression of flavonoid 3'-hydroxylase, flavonoid 3',5'-hydroxylase genes and related metabolite profiling of red cyanidin-/blue delphinidin-based anthocyanins in berry skin. BMC Genomics 7, 12. https://doi.org/10.1186/1471-2164-7-12.

Cenis, J.L., 1992. Rapid extraction of fungal DNA for PCR amplification. Nucleic Acids Res. 20 (9), 2380. https://doi.org/10.1093/nar/20.9.2380.

Chen, J.-C., et al., 2020. Diversity distributions and the anthocyanin associations of fungal endophytes in different colored grapevine leaves. J. Plant Biol. 63 (2), 107–116. https://doi.org/10.1007/s12374-020-09233-x.

Christen, D., Schonmann, S., Jermini, M., Strasser, R.J., Défago, G., 2007. Characterization and early detection of grapevine (*Vitis vinifera*) stress responses to esca disease by in situ chlorophyll fluorescence and comparison with drought stress. Environ. Exp. Bot. 60, 504–514. https://doi.org/10.1016/j.envexpbot.2007.02.003.

Collinge, D.B., Jensen, B., Jørgensen, H.J.L., 2022. Fungal endophytes in plants and their relationship to plant disease. Curr. Opin. Microbiol. 69, 102177. https://doi.org/10.1016/j.mib.2022.102177.

Csótó, A., et al., 2023. Hybrid *Vitis* cultivars with american or asian ancestries show higher tolerance towards grapevine trunk diseases. Plants 12 (2328), 1–16. https://doi.org/10.3390/plants12122328.

de Vries, S., Von Dahlen, J.K., Schnake, A., Ginschel, S., Schulz, B., Rose, L.E., 2018. Broad-spectrum inhibition of *phytophthora infestans* by fungal endophytes. FEMS. Microbiol. Ecol. 94, fiy037. https://doi.org/10.1093/femsec/fiy037.

Del Frari, G., Gobbi, A., Aggerbeck, M.R., Oliveira, H., Hansen, L.H., Ferreira, R.B., 2019. Characterization of the wood mycobiome of *Vitis vinifera* in a vineyard affected by esca. Spatial distribution of fungal communities and their putative relation with leaf symptoms. Front. Plant Sci. 10, 910. https://doi.org/10.3389/fpls.2019.00910.

Del Frari, G., Oliveira, H., Ferreira, R.B., 2021. White rot fungi (*Hymenochaetales*) and esca of grapevine: insights from recent microbiome studies. J. Fungi 7, 770. https://doi.org/10.3390/jof7090770.

Del Frari, G., Calzarano, F., Boavida, R., 2022. Understanding the control strategies effective against the esca leaf stripe symptom: the edge hypothesis. Phytopathol. Mediterr. 61 (1), 153–164. https://doi.org/10.36253/phyto-13295.

Del Frari, G., et al., 2023. Pruning wound protection products induce alterations in the wood mycobiome profile of grapevines. J. Fungi 9 (488). https://doi.org/10.3390/jof9040488.

Droby, S., Chalutz, E., Wilson, C.L., Wisniewski, M., Aug. 1989. Characterization of the biocontrol activity of *debaryomyces hansenii* in the control of *penicillium digitatum* on grapefruit. Can. J. Microbiol. 35 (8), 794–800. https://doi.org/10.1139/m89-132.

Dupont, P., et al., 2015. Fungal endophyte infection of ryegrass reprograms host metabolism and alters development. New Phytol. 208, 1227–1240. https://doi.org/10.1111/nph.13614.

Fan, Y., Gao, L., Chang, P., Li, Z., 2020. Endophytic fungal community in grape is correlated to foliar age and domestication. Ann. Microbiol. 70 (30). https://doi.org/10.1186/s13213-020-01574-9.

Feild, T.S., Lee, D.W., Holbrook, N.M., 2001. Why leaves turn red in autumn. The role of anthocyanins in senescing leaves of Red-Osier Dogwood. Plant Physiol. 127 (2), 566–574. https://doi.org/10.1104/pp.010063.

Feld, L., Nielsen, T.K., Hansen, L.H., Aamand, J., Albers, C.N., 2015. Establishment of bacterial herbicide degraders in a rapid sand filter for bioremediation of phenoxypropionate-polluted groundwater. Appl. Environ. Microbiol. 82 (3), 878–887. https://doi.org/10.1128/AEM.02600-15.

Ferrandino, A., Lovisolo, C., 2014. Abiotic stress effects on grapevine (*Vitis vinifera* L.): focus on abscisic acid-mediated consequences on secondary metabolism and berry quality. Environ. Exp. Bot. 103, 138–147. https://doi.org/10.1016/j.envexpbot.2013.10.012.

Ferrandino, A., Carra, A., Rolle, L., Schneider, A., Schubert, A., 2012. Profiling of hydroxycinnamoyl tartrates and acylated anthocyanins in the skin of 34 *Vitis vinifera* genotypes. J. Agric. Food Chem. 60 (19), 4931–4945. https://doi.org/10.1021/jf2045608.

Flamini, R., Mattivi, F., Rosso, M., Arapitsas, P., Bavaresco, L., 2013. Advanced knowledge of three important classes of grape phenolics: anthocyanins, stilbenes and flavonols. Int. J. Mol. Sci. 14 (10), 19651–19669. https://doi.org/10.3390/ijms141019651.

Fleurat-Lessard, P., et al., 2013. Differential occurrence of suberized sheaths in canes of grapevines suffering from black dead arm, esca or Eutypa dieback. Trees - Struct. Funct. 27 (4), 1087–1100. https://doi.org/10.1007/s00468-013-0859-z.

F. Fontaine et al., "Grapevine trunk diseases. A review", no. December, p. 25 pp, 2016. Available: http://www.oiv.int/public/medias/4650/trunk-diseases-oiv-2016.pdf.

Z.S.L. Foster, T. Sharpton, and N.J. Grunwald, "MetacodeR: an R package for manipulation and heat tree visualization of community taxonomic data from metabarcoding", *bioRxiv.*, vol. 13, no. 2, p. 071019, 2017, doi: 10.1101/071019.

Foster, Z.S.L., Chamberlain, S., Grünwald, N.J., 2018. Taxa: an R package implementing data standards and methods for taxonomic data. F1000Res. 7 (272), 272. https://doi.org/10.12688/f1000research.14013.1.

P. Gómez, A.G. Báidez, A. Ortuño, and J.A. Del Río, "Grapevine xylem response to fungi involved in trunk diseases", vol. 169, pp. 116–124, 2016, doi: 10.1111/aab.12285.

Gao, S., et al., 2016. ABF2, ABF3, and ABF4 promote ABA-mediated chlorophyll degradation and leaf senescence by transcriptional activation of chlorophyll catabolic genes and senescence-associated genes in *Arabidopsis*. Mol. Plant 9 (9), 1272–1285. https://doi.org/10.1016/j.molp.2016.06.006.

Gastou, P., Irvine, A.D., Arcens, C., Courchinoux, E., This, P., van Leeuwen, C., Delmas, C.E.L., 2024. Large gradient of susceptibility to esca disease revealed by long-term monitoring of 46 grapevine cultivars in a common garden vineyard. OENO One 58 (2). https://doi.org/10.20870/oeno-one.2024.58.2.8043.

Gaylarde, C., Ogawa, A., Beech, I., Kowalski, M., Baptista-Neto, J.A., 2017. Analysis of dark crusts on the church of Nossa Senhora do Carmo in Rio de Janeiro, Brazil, using chemical, microscope and metabarcoding microbial identification techniques. Int. Biodeterior. Biodegrad. 117 (January), 60–67. https://doi.org/10.1016/j.ibiod.2016.11.028.

Giauque, H., Connor, E.W., Hawkes, C.V., 2019. Endophyte traits relevant to stress tolerance, resource use and habitat of origin predict effects on host plants. New Phytol. 221, 2239–2249. https://doi.org/10.1111/nph.15504.

Gobbi, A., Santini, R., Filippi, E., Ellegaard-Jensen, L., Jacobsen, C.S., Hansen, L.H., 2019. Quantitative and qualitative evaluation of the impact of the G2 enhancer, bead sizes and lysing tubes on the bacterial community composition during DNA extraction from recalcitrant soil core samples based on community sequencing and qPCR. PLoS One 14 (e0200979). https://doi.org/10.1371/journal.pone.0200979.

Gobbi, A., Kyrkou, I., Filippi, E., Ellegaard-jensen, L., Hansen, L.H., 2020. Seasonal epiphytic microbial dynamics on grapevine leaves under biocontrol and copper fungicide treatments. Sci. Rep. 10, 681. https://doi.org/10.1038/s41598-019-56741-z.

Goufo, P., Cortez, I., 2020. A lipidomic analysis of leaves of esca-affected grapevine suggests a role for galactolipids in the defense response and appearance of foliar symptoms. Biology 9 (268), 1–23. https://doi.org/10.3390/biology9090268.

Goufo, P., Cortez, I., 2023. Changes in the relative abundance of fatty acids in grapevine leaves in response to esca complex disease. Acta Hortic. (1370), 121–128. https://doi.org/10.17660/ActaHortic.2023.1370.15.

Goufo, P., Singh, R.K., 2021. Metabolites differentiating asymptomatic and symptomatic grapevine plants (*Vitis vinifera* 'Malvasia-Fina') infected with esca complex disease-associated fungi. Biol. Life Sci. Forum 11 (27), 4–9. https://doi.org/10.3390/IECPS2021-11923.

Gramaje, D., Urbez-Torres, J.R., Sosnowski, M.R., 2018. Managing grapevine trunk diseases with respect to etiology and epidemiology: current strategies and future prospects. Plant Dis. 102 (1), 12–39. https://doi.org/10.1094/PDIS-04-17-0512-FE.

Guan, L., et al., 2012. Anthocyanin accumulation in various organs of a teinturier cultivar (*Vitis vinifera* L.) during the growing season. Am. J. Enol. Vitic. 63 (2), 177–184. https://doi.org/10.5344/ajev.2011.11063.

Guidoni, S., Mannini, F., Ferrandino, A., Argamante, N., Di Stefano, R., 1997. The effect of grapevine leafroll and rugose wood sanitation on agronomic performance and berry and leaf phenolic content of a nebbiolo clone (*Vitis vinifera* L.). Am. J. Enol. Vitic. 48 (4), 438–442. https://doi.org/10.5344/ajev.1997.48.4.438.

Gutha, L.R., Casassa, L.F., Harbertson, J.F., Naidu, R.A., Dec. 2010. Modulation of flavonoid biosynthetic pathway genes and anthocyanins due to virus infection in grapevine (*Vitis vinifera* L.) leaves. BMC Plant Biol. 10 (1), 187. https://doi.org/10.1186/1471-2229-10-187.

Hatier, J.-H.B., Gould, K.S., 2008. Anthocyanin function in vegetative organs. Anthocyanins. Springer New York, New York, NY, pp. 1–19. https://doi.org/10.1007/978-0-387-77335-3_1.

Hernandez-Montiel, L.G., Gutierrez-Perez, E.D., Murillo-Amador, B., Vero, S., Chiquito-Contreras, R.G., Rincon-Enriquez, G., 2018. Mechanisms employed by *Debaryomyces hansenii* in biological control of anthracnose disease on papaya fruit. Postharvest Biol. Technol. 139, 31–37. https://doi.org/10.1016/j.postharvbio.2018.01.015.

Hoch, W.A., Zeldin, E.L., McCown, B.H., Jan. 2001. Physiological significance of anthocyanins during autumnal leaf senescence. Tree Physiol. 21 (1), 1–8. https://doi.org/10.1093/treephys/21.1.1.

Hu, J., et al., 2023. p-coumaric acid prevents Colletotrichum gloeosporioides by inhibiting membrane targeting and organic acid metabolism. Postharvest Biol. Technol. 204, 112447. https://doi.org/10.1016/j.postharvbio.2023.112447.

Karácsony, Z., Mondello, V., Fontaine, F., Váczy, K.Z., 2023. The potential role of *Aureobasidium pullulans* in the development of foliar symptoms of Esca disease in grapevine. Oeno One 57 (3), 189–203. https://doi.org/10.20870/oeno-one.2023.57.3.7463.

Kedrina-okutan, O., et al., 2018. Constitutive polyphenols in blades and veins of grapevine (*Vitis vinifera* L.) healthy leaves. J. Agric. Food Chem. 66, 10977–10990. https://doi.org/10.1021/acs.jafc.8b03418.

Kernaghan, G., Mayerhofer, M., Griffin, A., Jul. 2017. Fungal endophytes of wild and hybrid *Vitis* leaves and their potential for vineyard biocontrol. Can. J. Microbiol. 63 (7), 583–595. https://doi.org/10.1139/cjm-2016-0740.

Knapp, G., Lázár, A., Molnár, A., Vajna, B., Karácsony, Z., Váczy, K.Z., Kovács, G.M., 2021. Above-ground parts of white grapevine *vitis vinifera* cv. Furmint share core members of the fungal microbiome. Environ. Microbiol. Rep. 13 (4), 509–520. https://doi.org/10.1111/1758-2229.12950.

Kobayashi, H., Suzuki, S., Tanzawa, F., Takayanagispi, T., 2009. Low expression of flavonoid 3',5'-hydroxylase (F3',5'H) associated with cyanidin-based anthocyanins in grape leaf. Am. J. Enol. Vitic. 60 (3), 362–367. https://doi.org/10.5344/ajev.2009.60.3.362.

Koljalg, U., et al., 2013. Towards a unified paradigm for sequence-based identification of fungi. Mol. Ecol. 22 (21), 5271–5277. https://doi.org/10.1111/mec.12481.

Kuntzmann, P., Villaume, S., Larignon, P., Bertsch, C., 2010. Esca, BDA and Eutypiosis: foliar symptoms, trunk lesions and fungi observed in diseased vinestocks in two vineyards in Alsace. Vitis - J. Grapevine Res. 49 (2), 71–76. https://doi.org/10.5073/vitis.2010.49.71-76.

L. Lahti, S. Sudarshan, and et al., "Tools for microbiome analysis in R. Microbiome package version 1.8.0".

Larignon, P., Dubos, B., 2001. Le Black Dead Arm. Maladie nouvelle à ne pas confondre avec l'esca. Phytoma- la Def. des végétaux 538, 26–29.

Larignon, P., Fulchic, R., Cere, L., Dubos, B., 2001. Observation on black dead arm in French vineyards. Phytopathol. Mediterr. 40 (Supplement), S336–S342.

Larignon, P., Coustou, I., Darné, G., Dubos, B., 2004. Les différences précoces dans la composition anthocyanique foliaire de Cabernet Sauvignon (*Vitis vinifera* L.) Atteint par l'esca ou par le black dead arm. In: 7. Symposium International d'oenologie de Bordeaux.

Larignon, P., Fontaine, F., Farine, S., Clément, C., Bertsch, C., 2009. Esca et Black Dead Arm: deux acteurs majeurs des maladies du bois chez la Vigne. Comptes Rendus - Biol. 332 (9), 765–783. https://doi.org/10.1016/j.crvi.2009.05.005.

Lecomte, P., Darrieutort, G., Defives, A., Louvet, Gwénaëlle, Liminana, J.-M., Blancard, D., 2006. Observations of Black Dead Arm symptoms in Bordeaux vineyards: evolution of foliar symptoms, localisation of longitudinal necroses, questions, hypotheses. In: "Integrated Protection in Viticulture" Proceedings of the meeting, pp. 20–22.

Lecomte, P., et al., 2012. new insights into esca of grapevine : the development of foliar symptoms and their association with xylem discoloration. Plant Dis. 96 (7), 924–934. https://doi.org/10.1094/PDIS-09-11-0776-RE.

Lev-Yadun, S., Gould, K.S., 2008. Role of anthocyanins in plant defence. Anthocyanins. Springer New York, New York, NY, pp. 22–28. https://doi.org/10.1007/978-0-387-77335-3_2.

Lima, M.R.M., et al., 2010. NMR metabolomics of esca disease-affected *Vitis vinifera* cv. Alvarinho leaves. J. Exp. Bot. 61 (14), 4033–4042. https://doi.org/10.1093/jxb/erq214.

Liu, D., Howell, K., 2020. Community succession of the grapevine fungal microbiome in the annual growth cycle. Environ. Microbiol. https://doi.org/10.1111/1462-2920.15172.

Magnin-Robert, M., et al., 2011. Leaf stripe form of esca induces alteration of photosynthesis and defence reactions in presymptomatic leaves. Funct. Plant Biol. 38 (11), 856–866. https://doi.org/10.1071/FP11083.

M. Magnin-robert, A. Spagnolo, A. Boulanger, C. Cl, E. Abou-mansour, and F. Fontaine, "Changes in plant metabolism and accumulation of fungal metabolites in response to esca proper and apoplexy expression in the whole grapevine", vol. 106, no. 6, pp. 541–553, 2016. doi: 10.1094/PHYTO-09-15-0207-R.

M. Magnin-robert et al., "Alterations in grapevine leaf metabolism occur prior to esca apoplexy appearance", vol. 30, no. 12, pp. 946–959, 2017, doi: 10.1094/MPMI-02-17-0036-R.

Margaria, P., Ferrandino, A., Caciagli, P., Kedrina, O., Schubert, A., Palmano, S., 2014. Metabolic and transcript analysis of the flavonoid pathway in diseased and recovered Nebbiolo and Barbera grapevines (*Vitis vinifera* L.) following infection by Flavescence dorée phytoplasma. Plant Cell Environ. 37 (9), 2183–2200. https://doi.org/10.1111/pce.12332.

Matus, J.T., et al., Jul. 2017. A group of grapevine MYBA transcription factors located in chromosome 14 control anthocyanin synthesis in vegetative organs with different specificities compared with the berry color locus. Plant J. 91 (2), 220–236. https://doi.org/10.1111/tpj.13558.

McCaig, M.L., et al., 2024. Response of stream habitat and microbiomes to spruce budworm defoliation: new considerations for outbreak management. Ecol. Appl. (May), 1–19. https://doi.org/10.1002/eap.3020.

McMurdie, P.J., Holmes, S., Apr. 2013. phyloseq: an R package for reproducible interactive analysis and graphics of microbiome census data. PLoS One 8 (4), e61217. https://doi.org/10.1371/journal.pone.0061217.

P.J. McMurdie and J.N. Paulson, "biomformat: an interface package for the BIOM file format." p. 19, 2016.

Medina-Córdova, N., Rosales-Mendoza, S., Hernández-Montiel, L.G., Angulo, C., Jun. 2018. The potential use of *debaryomyces hansenii* for the biological control of pathogenic fungi in food. Biol. Control 121, 216–222. https://doi.org/10.1016/j.biocontrol.2018.03.002.

Merzlyak, M.N., Chivkunova, O.B., Solovchenko, A.E., Naqvi, K.R., 2008. Light absorption by anthocyanins in juvenile, stressed, and senescing leaves. J. Exp. Bot. 59 (14), 3903–3911. https://doi.org/10.1093/jxb/ern230.

Molnár, A., et al., 2022. Physiological parameters and leaf and berry mycobiome composition. Plants 22 (1924).

Mondello, V., et al., 2018. Grapevine trunk diseases: a review of fifteen years of trials for their control with chemicals and biocontrol agents. Plant Dis. 102 (7), 1189–1217. https://doi.org/10.1094/PDIS-08-17-1181-FE.

Mugnai, L., Graniti, A., Surico, G., 1999. Esca (black measles) and brown wood-streaking: two old and elusive diseases of grapevines. Plant Dis. 83 (5), 404–418. https://doi.org/10.1094/PDIS.1999.83.5.404.

Murakami, P.F., Schaberg, P.G., Shane, J.B., 2008. Stem girdling manipulates leaf sugar concentrations and anthocyanin expression in sugar maple trees during autumn. Tree Physiol. 28 (10), 1467–1473. https://doi.org/10.1093/treephys/28.10.1467.

Nascimento, R., et al., 2019. Plant physiology and biochemistry early stage metabolic events associated with the establishment of *Vitis vinifera* – *Plasmopara viticola* compatible interaction. Plant Physiol. Biochem. 137, 1–13. https://doi.org/10.1016/j.plaphy.2019.01.026.

Negro, C., et al., 2020. Biochemical changes in leaves of *Vitis vinifera* cv. Sangiovese infected by Bois Noir phytoplasma. Pathogens. 9 (4), 269. https://doi.org/10.3390/pathogens9040269.

Nguyen, T.L.A., Bhattacharya, D., 2022. antimicrobial activity of quercetin: an approach to its mechanistic principle. Molecules. 27 (8). https://doi.org/10.3390/molecules27082494.

J. Oksanen et al., "Vegan: community ecology package. R package version 2.0-10", http://CRAN.R-project.org/package=vegan. 2013.

Pan, X., et al., 2020. The symbioses of endophytic fungi shaped the metabolic profiles in grape leaves of different varieties. PLoS One 15 (9), e0238734. https://doi.org/10.1371/journal.pone.0238734.

Papadopoulou, E., Bekris, F., Vasileiadis, S., Papadopoulou, K.K., Karpouzas, D.G., Dec. 2022. Different factors are operative in shaping the epiphytic grapevine microbiome across different geographical scales: biogeography, cultivar or vintage? J. Sustain. Agric. Environ. 1 (4), 287–301. https://doi.org/10.1002/sae2.12030.

Peng, M., et al., 2008. Adaptation of Arabidopsis to nitrogen limitation involves induction of anthocyanin synthesis which is controlled by the NLA gene. J. Exp. Bot. 59 (11), 2933–2944. https://doi.org/10.1093/jxb/ern148.

Pinto, C., Pinho, D., Sousa, S., Pinheiro, M., Egas, C., Gomes, A.C., 2014. Unravelling the diversity of grapevine microbiome. PLoS One 9 (1), e85622. https://doi.org/10.1371/journal.pone.0085622.

Pirie, A., Mullins, M.G., 1976. Changes in anthocyanin and phenolics content of grapevine leaf and fruit tissues treated with sucrose, nitrate, and abscisic acid. Plant Physiol. 58 (4), 468–472. https://doi.org/10.1104/pp.58.4.468.

Rantsiou, K., et al., 2020. Impact of chemical and alternative fungicides applied to grapevine cv nebbiolo on microbial ecology and chemical-physical grape characteristics at harvest. Front. Plant Sci. 11, 1–16. https://doi.org/10.3389/fpls.2020.00700.

Serra, S., Ligios, V., Schianchi, N., Prota, V.A., Scanu, B., 2018. Expression of grapevine leaf stripe disease foliar symptoms in four cultivars in relation to grapevine phenology and climatic conditions. Phytopathol. Mediterr. 57 (3), 557–568. https://doi.org/10.14601/Phytopathol_Mediterr-24088.

Singh, P., Gobbi, A., Santoni, S., Hansen, L.H., This, P., Péros, J., 2018a. Assessing the impact of plant genetic diversity in shaping the microbial community structure of *Vitis vinifera* phyllosphere in the Mediterranean. Front. Life Sci. 11 (1), 35–46. https://doi.org/10.1080/21553769.2018.1552628.

Singh, P., Santoni, S., This, P., Péros, J.-P., 2018b. Genotype-environment interaction shapes the microbial assemblage in grapevine's phyllosphere and carposphere: an NGS approach. Microorganisms. 6, 96. https://doi.org/10.3390/microorganisms6040096.

Solfanelli, C., Poggi, A., Loreti, E., Alpi, A., Perata, P., 2006. Sucrose-specific induction of the anthocyanin biosynthetic pathway in *Arabidopsis*. Plant Physiol. 140 (2), 637–646. https://doi.org/10.1104/pp.105.072579.

Spagnolo, A., et al., 2012. Physiological changes in green stems of *Vitis vinifera* L . cv . Chardonnay in response to esca proper and apoplexy revealed by proteomic and transcriptomic analyses. J. Proteome Res. 461–475. https://doi.org/10.1021/pr200892g.

Sumby, K.M., Caliani, N.S., Jiranek, V., 2021. Yeast diversity in the vineyard: how it is defined, measured and influenced by fungicides. Aust. J. Grape Wine Res. 27 (2), 169–193. https://doi.org/10.1111/ajgw.12479.

Surico, G., Mugnai, L., Marchi, G., 2006. Older and more recent observations on esca: a critical overview. Phytopathol. Mediterr. 45 (SUPPL. 1), 68–86. https://doi.org/10.14601/PHYTOPATHOL_MEDITERR-1847.

Surico, G., 2009. Towards a redefinition of the diseases within the esca complex of grapevine. Phytopathol. Mediterr. 48 (1), 5–10.

Tattini, M., et al., 2005. On the role of flavonoids in the integrated mechanisms of response of *Ligustrum vulgare* and *Phillyrea latifolia* to high solar radiation. New Phytol. 167 (2), 457–470. https://doi.org/10.1111/j.1469-8137.2005.01442.x.

Tattini, M., et al., 2014. Epidermal coumaroyl anthocyanins protect sweet basil against excess light stress: multiple consequences of light attenuation. Physiol. Plant 152 (3), 585–598. https://doi.org/10.1111/ppl.12201.

Teng, S., Keurentjes, J., Bentsink, L., Koornneef, M., Smeekens, S., 2005. Sucrose-specific induction of anthocyanin biosynthesis in *Arabidopsis* requires the MYB75/PAP1 gene. Plant Physiol. 139 (4), 1840–1852. https://doi.org/10.1104/pp.105.066688.

Úrbez-Torres, J.R., 2011. The status of *Botryosphaeriaceae* species infecting grapevines. Phytopathol. Mediterr. 50 (SUPPL), 5–45. https://doi.org/10.14601/Phytopathol_Mediterr-9316.

P.M. Valero-Mora, *ggplot2: elegant graphics for Data analysis*, vol. 35, 2015. doi: 10.18637/jss.v035.b01.

Valtaud, C., Foyer, C.H., Fleurat-lessard, P., Bourbouloux, A., 2009. Systemic effects on leaf glutathione metabolism and defence protein expression caused by esca infection in grapevines. Funct. Plant Biol. 36, 260–279. https://doi.org/10.1071/FP08293.

Valtaud, C., Thibault, F., Larignon, P., Bertsch, C., Fleurat, P., Bourbouloux, A., 2011. Systemic damage in leaf metabolism caused by esca infection. Aust. J. Grape Wine Res. 17, 101–110. https://doi.org/10.1111/j.1755-0238.2010.00122.x.

Vaz, A.T., Del Frari, G., Chagas, R., Oliveira, H., Ferreira, R.Boavida, 2020. Precise nondestructive location of defective woody tissue in grapevines affected by wood diseases. Phytopathol. Mediterr. 59 (3), 441–451. https://doi.org/10.14601/Phyto-11110.

Viala, P., 1926. Recherces sur les maladies de la vigne. Esca. Ann. des Épiphyties Phytogénétique 12, 5–108.

Ważny, R., et al., 2021. The effect of endophytic fungi on growth and nickel accumulation in *Noccaea* hyperaccumulators. Sci. Total. Environ. 768 (768), 144666. https://doi.org/10.1016/j.scitotenv.2020.144666.

A.Y. Wang, U. Naumann, S. Wright, D. Eddelbuettel, D. Warton, and S. Wright, "Mvabund: statistical methods for analysing multivariate abundance data." pp. 1–95, 2017.

Weiller, F., et al., 2024. Metabolomic analysis of grapes and leaves from symptomatic and asymptomatic *Vitis vinifera* grapevines with Esca disease. Curr. Plant Biol. https://doi.org/10.1016/j.cpb.2024.100378.

Weiss, D., 2000. Regulation of flower pigmentation and growth: multiple signaling pathways control anthocyanin synthesis in expanding petals. Physiol. Plant 110, 152–157. https://doi.org/10.1034/j.1399-3054.2000.110202.x.

Wickham, H., et al., Nov. 2019. Welcome to the Tidyverse. J. Open. Source Softw. 4 (43), 1686. https://doi.org/10.21105/joss.01686.

S. Xie, Y. Lei, H. Chen, J. Li, and H. Chen, "R2R3-MYB transcription factors regulate anthocyanin biosynthesis in grapevine vegetative tissues", vol. 11, pp. 1–12, 2020, doi: 10.3389/fpls.2020.00527.

Yang, Y.Z., et al., 2022. Physicochemical and biotic changes and the phylogenetic evenness of microbial community in soil subjected to phytoreclamation. Microb. Ecol. 84 (4), 1182–1194. https://doi.org/10.1007/s00248-021-01890-w.

Yu, M., et al., 2020. Exposure to endophytic fungi quantitatively and compositionally alters anthocyanins in grape cells. Plant Physiol. Biochem. 149, 144–152. https://doi.org/10.1016/j.plaphy.2020.02.006.

Zhao, Y., et al., 2016. ABA receptor PYL9 promotes drought resistance and leaf senescence. Proc. Natl. Acad. Sci. U.S.A. 113 (7), 1949–1954. https://doi.org/10.1073/pnas.1522840113.